HHS Public Access

Author manuscript

Cell Rep. Author manuscript; available in PMC 2024 September 14.

Published in final edited form as:

Cell Rep. 2024 August 27; 43(8): 114621. doi:10.1016/j.celrep.2024.114621.

Epithelial organoid supports resident memory CD8 T cell differentiation

Max R. Ulibarri[1,8], **Ying Lin**[1,2,8], **Julian C. Ramprashad**[1], **Geongoo Han**[1], **Mohammad H. Hasan**[1], **Farha J. Mithila**[1,3], **Chaoyu Ma**[4], **Smita Gopinath**[5], **Nu Zhang**[4,6], **J. Justin Milner**[7], **Lalit K. Beura**[1,9,*]

[1]Department of Molecular Microbiology and Immunology, Brown University, Providence, RI 02912, USA

[2]Pathobiology Graduate Program, Brown University, Providence, RI 02912, USA

[3]Molecular Biology, Cell Biology and Biochemistry Graduate Program, Brown University, Providence, RI 02912, USA

[4]Department of Microbiology, Immunology and Molecular Genetics, University of Texas Health Science Center, San Antonio, TX 78229, USA

[5]Department of Immunology and Infectious Diseases, Harvard T.H. Chan School of Public Health, Cambridge, MA 02115, USA

[6]South Texas Veterans Health Care System, San Antonio, TX 78229, USA

[7]Department of Microbiology and Immunology, University of North Carolina, Chapel Hill, NC 27599, USA

[8]These authors contributed equally

[9]Lead contact

SUMMARY

Resident memory T cells (TRMs) play a vital role in regional immune defense. Although laboratory rodents have been extensively used to study fundamental TRM biology, poor isolation efficiency and low cell survival rates have limited the implementation of TRM-focused high-throughput assays. Here, we engineer a murine vaginal epithelial organoid (VEO)-CD8 T cell

*Correspondence: lalit_beura@brown.edu.

AUTHOR CONTRIBUTIONS

Conceptualization, M.R.U., Y.L., and L.K.B.; methodology and reagents, C.M., S.G., N.Z., and J.J.M.; experimentation, M.R.U., Y.L., J.C.R., G.H., M.H.H., F.J.M., and L.K.B.; data analysis, M.R.U., J.C.R., Y.L., and L.K.B.; writing, M.R.U., Y.L., J.C.R., and L.K.B.; funding acquisition, L.K.B.

DECLARATION OF INTERESTS

The authors declare no competing interests.

DECLARATION OF GENERATIVE AI AND AI-ASSISTED TECHNOLOGIES IN THE WRITING PROCESS

During the preparation of this work, the authors used ChatGPT to check grammatical issues and improve sentence structure within the "introduction" section. After using this tool, the authors reviewed and edited the content as needed and take full responsibility for the content of the publication.

SUPPLEMENTAL INFORMATION

Supplemental information can be found online at https://doi.org/10.1016/j.celrep.2024.114621.

co-culture system that supports CD8 TRM differentiation. These *in-vitro*-generated TRMs are phenotypically and transcriptionally similar to *in vivo* TRMs. Pharmacological and genetic approaches showed that transforming growth factor β (TGF-β) signaling plays a crucial role in their differentiation. The VEOs in our model are susceptible to viral infections and the CD8 T cells are amenable to genetic manipulation, both of which will allow a detailed interrogation of antiviral CD8 T cell biology. Altogether we have established a robust *in vitro* TRM differentiation system that is scalable and can be subjected to high-throughput assays that will rapidly add to our understanding of TRMs.

In brief

Technical issues with resident memory T cell (TRM) isolation and survival have hindered detailed inquiries into TRM biology. Ulibarri et al. establish a vaginal epithelial organoid (VEO)-CD8 T cell co-culture system that enables epithelial TRM differentiation *in vitro*. This co-culture model will expand fundamental and translational mucosal TRM research.

Graphical Abstract

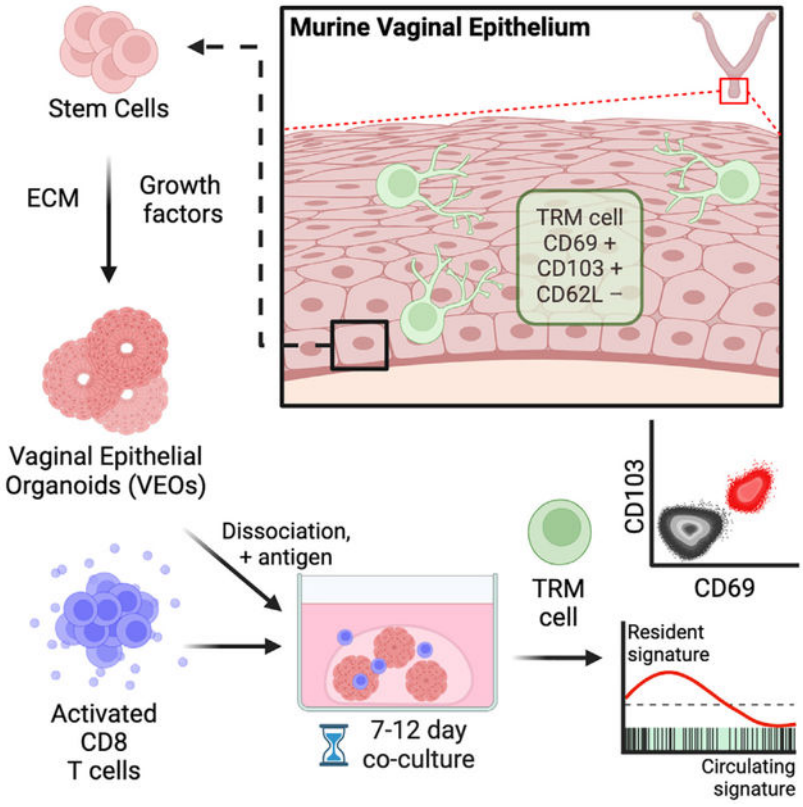

INTRODUCTION

Memory CD8 T cells play a crucial role in coordinating the immune response against intracellular infections and malignancies. Their duties, however, are compartmentalized, with distinct subsets of memory CD8 T cells performing surveillance responsibilities

depending on their anatomic location. Specifically, circulating memory CD8 T cells, which encompass both central memory (TCMs) and effector memory CD8 T cells (TEMs), continuously patrol the bloodstream and secondary lymphoid organs (SLOs), such as the spleen and lymph nodes. Additionally TEMs also survey non-lymphoid tissues (NLTs).[1,2] Resident memory CD8 T cells (TRMs), by contrast, are stationed within specific tissues and do not routinely recirculate through blood or lymphatics. However, TRMs upon restimulation can join the circulating memory T cell pool and differentiate into TEMs and TCMs.[3–5] The front-line placement of TRMs positions them as the first line of defense against invading pathogens. Upon contact with infected antigen-presenting cells, TRMs promptly release a milieu of cytokines and chemokines and exhibit cytotoxic capacity. This multifaceted response serves to curtail pathogen replication, alert the immune system, and recruit other immune cells to the site of infection. Consequently, the presence of TRMs is correlated with expedited pathogen control in a number of barrier tissues.[6,7]

Localizing abundant quantities of antiviral CD8 TRMs in these tissues is associated with a rapid protective benefit in infection.[8–10] Accordingly, positioning a robust TRM population in barrier tissues that is maintained long term is a crucial vaccination goal. This requires an in-depth understanding of the signals that mediate the differentiation of naive CD8 T cells to TRMs. While the identities of certain core transcription factors (e.g., Ho-bit, Blimp-1, Runx3, and KLF2) and surface molecules (e.g., CD103, CD69, and CD49a) have been discovered, our understanding of the TRM differentiation process is far from complete.[11–13] TRM development is complex and involves multiple anatomical niches, including initial effector differentiation in SLOs, trafficking via blood, and final TRM formation at the tissue of residence under the influence of the local microenvironment. The contribution of the local tissue-specific signals in dictating TRM fate is an intense area of research, as the information could be used to modulate TRM density in an organ-restricted manner. Many of these studies employ gene-specific knockout (KO) mice and transgenic CD8 T cells to elucidate mechanistic insights into the signaling mechanism that induces TRMs. However, a major issue remains in distinguishing the roles of specific genes in the initial CD8 T cell effector differentiation process, which occurs in SLOs, from their contributions to the subsequent differentiation process that transpires within the respective non-lymphoid barrier tissues once the T cells have homed there. The utility of tissue-specific Cre-driver lines, which can be temporally induced, is constrained by their limited availability and their susceptibility to spurious or leaky induction. Further-more, these *in vivo* animal studies are not well suited for high-throughput assays and are restricted in their capacity for invasive experimental manipulations. Addressing these limitations, organoid models have emerged as a reductionist surrogate system that overcomes the shortcomings of *in vivo* models while retaining the three-dimensional (3D) architecture and function of the target tissues.[14,15]

Epithelial organoids can be derived from induced pluripotent stem cells or adult epithelial stem cells. They are phenotypically stable through successive passages, which makes them an efficacious alternative to *in vivo* assays.[16,17] Enteric and lung organoids have been well established and currently offer tremendous prospects for fundamental biologic discovery as well as personalized medicine. In comparison, organs with type II mucosa have been less investigated. Here, we exploited a recently established model of vaginal epithelial organoids (VEOs)[18] to dissect the localized interactions between T cells and the vaginal epithelium

and study TRM differentiation. By co-culturing activated CD8 T cells with VEOs, we successfully induced CD8 TRM differentiation. Subsequent analysis of the transcriptome and phenotype of the CD8 T cells showed robust alignment of the *in-vitro*-generated TRMs with bona fide *in vivo* CD8 TRMs. This reductionist model system enables in-depth exploration of the intricate inter-play between T cells and the vaginal epithelium, providing valuable insights into the local differentiation of TRMs within the FRT.

RESULTS

Establishment of VEO-CD8 T cell co-culture system

In this study, we employed a VEO generation system, as previously outlined by Ali et al. in 2020,[19] to cultivate VEOs (Figure 1A). Single-cell suspensions of epithelial cells were embedded in basement membrane extract (BME) and cultured in a growth medium designed for the maintenance and proliferation of epithelial stem cells.[20] These VEOs were successfully maintained for at least 21 days through supplementation of fresh medium, during which they steadily grew in size (Figure 1B). Notably, in differential interference contrast images, the organoids exhibited a distinct darker core and a lighter external boundary composed of a basal layer of epithelial cells (Figure 1B). We also measured the relative transcript levels of various genes associated with the different layers of the vaginal epithelium at different times post-culture. Transcripts associated with stem cells (*Axin2*) and proliferation (*Birc5*, *Ki67*) were more abundant at earlier times (day 5 post-culture), whereas genes associated with luminal keratinocytes (*Sprr1a*) and cornified cells (*Krt1*) increased at later times (Figure 1C).[18,20] Our histological analysis of the VEOs demonstrated consistent staining with the pan-epithelial cell marker Ep-cam. Most proliferating cells ($Ki67^+$) were in the outer layer (Figure 1D, top row). Similarly, the basal epithelial cell marker keratin-5 was predominantly localized to the outermost layer of cells within the organoids (Figure 1D, middle row). We also detected prominent expression of P63, a marker associated with the basal and parabasal layers of the vaginal squamous epithelium on the outer two layers of VEOs (Figure 1D, bottom row).[21]

Next, we aimed to introduce CD8 T cells into the VEOs to test whether exposure to VEO-derived cues could facilitate CD8 T cell differentiation into mature tissue TRMs. To achieve this, naive monoclonal T cell receptor (TCR) transgenic CD8 T cells were activated as described before.[22] The expanded CD8 T cells were then co-cultured with the VEOs in the presence of interleukin (IL)-2, as shown in Figure 1A, and their presence within the BME was imaged using a congenic marker (CD90.1) through confocal microscopy. CD8 T cells were observed near fully developed organoids and found scattered around the organoids, as presented in Figure 1E. These CD8-VEO co-cultures were successfully maintained for a minimum of 16 days with regular medium changes, supplemented with IL-2 and other organoid-specific growth factors. Provision of IL-2 was important for the survival of CD8 T cells, as co-cultures maintained in the absence of IL-2 lost most of their CD8 T cells by day 10. In summary, we established VEOs that closely resemble previously described organoids and effectively introduced CD8 T cells into the VEO environment for further investigation.

CD8 T cells acquire an epithelial TRM phenotype upon co-culture with VEOs

Following the successful maintenance of CD8 T cells with VEOs, we performed phenotypic characterizations of these co-cultured CD8 T cells. Expression of various CD8 T cell-specific markers was assessed from dissociated VEO-CD8 co-cultures via flow cytometry. CD8 T cells maintained alone in the absence of VEOs upregulated CD103 but not CD69, and few cells expressed both CD69 and CD103 (Figure 2A, top row). In contrast, a substantial proportion (~40%–65%) of the co-cultured CD8 T cells showed dual expression of CD69 and CD103 (Figure 2A, middle row). This double-positive CD8 TRM population is normally observed in the epithelial compartment.[23–25] Importantly, this *in vitro* co-cultured CD8 T cell phenotype resembled that of antiviral CD8 TRMs generated against murine HSV-2 infection *in vivo* (Figure 2A, bottom row). These CD8 T cells are well documented as bona fide residents within the vaginal and cervical tissues.[26,27] Beyond CD69 and CD103, the co-cultured CD8 T cells also adopted other phenotypic attributes of TRMs, including downregulation of Ly6C and CD62L and upregulation of PD-1.[23,28] The interaction of TRMs with extracellular matrix (ECM) components is important for many aspects of TRM biology.[29,30] To test if the acquisition of the TRM phenotype was influenced by the presence of BME, which provides a 3D environment and support for the growth and maintenance of VEOs, we cultured CD8 T cells within the BME in the absence of VEOs. Even after 12 days of culture, these CD8 T cells failed to adopt a $CD69^{+}CD103^{+}$ TRM phenotype, confirming that ECM alone cannot drive the TRM phenotype and that VEOs are crucial in driving TRM formation (Figures S1A and S1B). Additionally, co-cultured CD8 T cells exhibited downregulation of the transcription factors T-bet and Eomes, aligning with established TRM traits (Figure S1C).[31] We further tested if the passage history of the organoids can influence their TRM induction abilities. VEOs at passage 18 were equally capable of generating $CD69^{+}CD103^{+}$ CD8 T cells as those at passage 8, suggesting no erosion of TRM induction ability with increasing passages (Figures S1D and S1E).

To gain insight into the kinetics of acquisition of various TRM markers, we conducted longitudinal phenotyping of co-cultured CD8 T cells, revealing that CD103 upregulation occurs at a faster rate compared to CD69 *in vitro* (Figures S2A and S2B). We further performed deeper phenotypic characterization of these different CD8 populations generated via co-culture. This revealed that the $CD69^{+}CD103^{+}$ CD8 T cells conform to the established true TRM phenotype ($CD62L^{lo}$, $P2rx7^{hi}$, $CXCR6^{hi}$) and express CD49a as well as the cytotoxic molecule granzyme B (Figure S2C). However, the $CD69^{-}CD103^{+}$CD8 T cells failed to adopt these TRM phenotypes and rather resembled circulating CD8 T cells expressing higher levels of CD62L. So, our future analyses were focused on the $CD69^{+}CD103^{+}$ T cells.

Previous studies in mouse models have suggested that a local second antigenic encounter in the target tissue can enhance the differentiation of effector CD8 T cells into TRMs.[32,33] In our study, we aimed to replicate this process by exposing the activated CD8 T cells to VEOs presenting cognate antigen. For this, disaggregated epithelial cells from VEOs were incubated with cognate antigenic peptide ($GP_{33–41}$ for P14 CD8 T cells and $gB_{498–505}$ for gBT-I CD8 T cells) for an hour and subsequently washed to eliminate any unbound peptides

(Figure 2B). Peptide-loaded epithelial cells were incubated with activated CD8 T cells and embedded together in BME to induce VEO formation and TRM differentiation. The antigen-exposed CD8 T cells exhibited a significantly higher percentage of $CD69^+CD103^+$ TRMs, as depicted in Figures 2C and 2D, as early as 8 days in comparison to the non-antigen-exposed CD8 T cells. The expression of other TRM-associated markers was also more pronounced in these cells (Figures 2C and 2D). In summary, we have successfully differentiated CD8 TRMs through VEO-derived signals, and this process was enhanced by a transient second antigen exposure.

Transcriptional alignment of *in-vitro*-generated TRMs with bona fide *in vivo* TRMs

The phenotypic resemblance between VEO-induced CD8 TRMs and CD8 TRMs established *in vivo* upon viral infection strongly suggests that the *in vitro* generated $CD69^+CD103^+$ CD8 T cells faithfully resemble TRMs. However, a number of these phenotypic markers can arise during T cell activation and cytokine stimulation and have led to questioning the establishment of TRM identity by phenotyping alone. Detailed transcriptional analyses of TRMs across tissues and species have established a core-TRM transcriptional signature that has been used to establish the fidelity and identity of particular TRM populations.[28,34] We performed population-based RNA sequencing analysis comparing the $CD69^+CD103^+$ *in-vitro*-generated CD8 T cell subset with CD8 T cells maintained without the VEOs. Out of the 6,223 (3,748 up- and 2,475 downregulated) differentially expressed genes between the 2 cell types, many of the top 25 up- and downregulated genes (e.g., upregulated: *Gzma*, *Hic1*, *Ccr9*, and *Itgae*; downregulated: *Eomes*, *Sell*, *Klf2*, and *S1pr1*) are similarly regulated in bona fide TRMs (Figure 3A).[11,13,35] To further substantiate this overlap, we generated transcriptomics profiles of FRT $CD103^+$ CD8 TRMs and splenic CD8 TCMs from HSV-2 memory mice. We compared the expression of a selected list of genes associated with various T cell processes between these *in vivo* CD8 T cells and the VEO-induced CD8 T cells. A heatmap depicting the expression of these genes between co-cultured CD8 T cells and CD8 T cells cultured alone is shown in Figure 3B. Expression of these same genes between bona fide FRT TRMs and splenic TCMs is shown on the right (Figure 3B).

The *in vitro* TRMs exhibited differential expression of several transcription factors associated with enforcing residency, such as the downregulation of *Tcf7*, *Klf2*, and *Eomes* and the upregulation of *Runx3*, *Bhlhe40*, and *Prdm1*. Similarly, many of the genes associated with migration (e.g., *Sell*, *Ccr7*, and several other chemokine receptors) were downregulated in *in vitro* TRMs as well as *in-vivo*-established TRMs (Figure 3B). However, integrin and cadherins that help anchor TRMs to local tissues (e.g., *Itgae*, *Cdh1*, and *Itga1*) were upregulated in both *in vitro* and *in vivo* TRMs. A gene set enrichment analysis found significant enrichment of core TRM signature genes (extracted from publicly available data)[34] in the *in vitro* TRMs and negative enrichment of genes associated with circulating CD8 T cells (Figure 3C). A further analysis of biological processes overrepresented in the co-cultured TRMs within the MSigDB database showed enrichment of several pathways upregulated in memory CD8 T cells compared to naive CD8 T cells (Figure 3D). Interestingly, we also noticed genes upregulated in response to retinoic

acid and transforming growth factor β (TGF-β) are represented among these pathways. In summary, our transcriptomic analysis showed a strong overlap of various TRM gene signatures between the *in-vitro*- and *in-vivo*-generated CD8 TRMs, further verifying their TRM identity.

Reactivated circulating memory CD8 T cells can differentiate into TRMs under the influence of VEOs

After establishing that VEOs can support differentiation of effector CD8 T cells (generated from the activation of naive CD8 T cells) into mature TRMs *in vitro* with remarkable efficiency, we tested whether they could also facilitate TRM differentiation of circulating memory CD8 T cells. For this, we first generated TCMs and TEMs *in vivo* by transferring naive congenically marked P14 CD8 T cells ($CD45.1^+$) to C57BL/6J mice, followed by LCMV infection. The P14 CD8 T cells were allowed to differentiate into circulating memory CD8 T cells for 75 days post-infection, at which point the SLOs from these mice were isolated and TCMs ($CD45.1^+$, $CD44^{hi}$, $CD62L^{hi}$) as well as TEMs ($CD45.1^+$, $CD44^{hi}$, $CD62L^{lo}$) were separated by flow sorting. Sorted TCMs and TEMs were co-cultured with VEOs to induce differentiation for 10 days. As a positive control, we also included *in-vitro*-generated effector CD8 T cells, which have been shown to differentiate into $CD69^+CD103^+$ TRMs. Although a fraction of TCMs and TEMs survived in co-culture, they failed to adopt the epithelial TRM phenotype (Figures 4A and 4B). In contrast, TCMs and TEMs exposed to VEOs loaded with cognate antigenic peptide (gp33) formed TRM-like cells (Figures 4A and 4B). This suggests that circulating memory CD8 T cells require antigenic restimulation to enable their differentiation into TRMs. However, the efficiency of adoption of various TRM-associated markers ($CD69^+CD103^+$, $CXCR6^+$, and $CD62L^-$) was significantly lower among the reactivated TCMs and TEMs than effector CD8 T cells (Figure 4B). The CD8 TCMs showed better acquisition of the TRM phenotype compared to TEMs, although this difference was not statistically significant. Altogether these results suggest that circulating memory CD8 T cells can be programmed into TRMs but need reactivation for differentiation.

VEO-induced CD8 TRMs remain functional and can be generated in the absence of physical contact with the organoids

TRMs located in frontline mucosal tissues rapidly elicit cytotoxic granules and cytokines after TCR stimulation, and maintenance of this functionality is crucial to limit pathogen replication. Here, we assessed whether the *in-vitro*-generated CD8 TRMs remain functional in response to antigenic recall. For this, wells containing CD8 TRMs and VEOs (14 days post-co-culture) were treated with an antigenic peptide in the presence of brefeldin A, and the expression of various cytokine molecules was checked by intra-cellular cytokine staining followed by flow cytometry. As shown in Figures 5A and 5B, CD8 T cells elaborated significant amounts of interferon-g, tumor necrosis factor alpha (TNF-α), and IL-2 in response to the peptide challenge. These data indicate that TRMs generated in response to VEO-derived cues retain their functional potential, as has been shown for *in vivo* TRMs.[10]

Next, we tested if the *in vitro* TRM differentiation process relies on direct interaction with VEOs or can be achieved when the VEOs and CD8 T cells are physically separated. For

this, we used Transwell inserts containing semipermeable membranes such that the CD8 T cells can access any soluble factors produced by the VEOs but are not in direct contact. We exposed the CD8 T cells to VEOs through the semipermeable barrier for up to 15 days and evaluated the CD8 T cell phenotype by flow cytometry. Interestingly, these CD8 T cells upregulated the classical TRM markers CD69 and CD103 (Figures 5C and 5D). For comparison, we also had wells without the Transwell inserts where CD8 T cells were either maintained alone or embedded in the VEO co-culture system. As expected, the co-cultured CD8 T cells upregulated TRM-associated markers. These results showed that TRM differentiation can be mediated by the soluble factors produced by epithelial organoids. We next asked whether induction of the TRM phenotype can be achieved through regular supplementation of conditioned medium (CM) from wells containing VEOs. Exposure of effector CD8 T cells to VEO-derived CMs (every 2 days for 10 days) did not dramatically upregulate CD69 or CD103 expression (Figure 5E). Embedding the CD8 T cells in BME also failed to induce a TRM phenotype. Altogether these data suggest that while *in vitro* TRM differentiation can be induced by soluble agents, these factors might be labile in nature and require continuous contact with responding CD8 T cells to generate $CD69^{+}CD103^{+}$ CD8 T cells.

VEOs support viral replication, and the organoid co-culture system can be used to probe molecular drivers of antiviral TRM differentiation

The vaginal epithelium is a common portal for viral invasion and often serves as an initial replication site before the pathogen spreads to distal organs. As such, understanding the viral replication dynamics in the vaginal mucosa and the ensuing immune response is crucial to improve antiviral therapies and vaccines. Here, we aimed to test whether VEOs can be targeted by a common sexually transmitted infection, HSV. For this, we exposed mature VEOs to recombinant HSV-1 and HSV-2 viruses encoding green fluorescent reporter protein. The HSV-1 K26GFP encodes a green fluorescent VP26 capsid protein.[36] Infected cells showed punctate green signals, which correspond to capsid assembly sites within the nucleus between 24 and 36 h post-infection (Figure 6A, middle row).[36] The HSV-2(333)ZAG-GFP expresses GFP under the control of a cytomegalovirus promoter; the CMV-GFP construct was inserted in an intergenic region between UL3 and UL4 of HSV-2.[37] Here, the GFP signals were found to be more diffused across the whole infected organoids (Figure 6A, bottom row). These findings together suggest that intact VEOs can support HSV-1/−2 replication.

Next, we wanted to test if the *in vitro* VEO-mediated CD8 TRM differentiation system could be used to define regulators of TRM fate. Notably, we detected elevated expression of the transcription factor Runx3 in VEO-co-cultured CD8 T cells compared with the CD8 T cells alone (Figure 3B). Runx3 has also been established as a key transcription factor that promotes TRM formation in the intestine.[12] To test whether Runx3 influences FRT TRM formation, we transduced activated CD8 T cells with either a Runx3-encoding retrovirus (simultaneously encoding an EGFP reporter) or a control vector encoding mCherry. Transduced CD8 T cells were mixed at 1:1 ratio and co-cultured with the VEOs for 5–10 days. We found a significantly higher percentage of $CD69^{+}CD103^{+}$ TRMs among the Runx3 transduced cells compared to the control vector (Figures 6B and 6C). These

data suggest that Runx3 potentiates FRT CD8 TRM formation, and more importantly, our findings establish a proof of principle that the VEO-CD8 co-culture system can be used to identify molecular regulators of TRM differentiation.

A critical advantage of the *in vitro* differentiation system is the generation of an abundant (near unlimited) number of TRMs compared to the sparse number of TRMs that can be isolated from the FRT *in vivo*.[38] A comparison of the relative TRM yield between the two systems showed that a single well of a 96-well plate could generate ~3 times more CD8 TRMs than what could be extracted from a single mouse lower FRT that was infected with LCMV intravaginally 30 days prior (Figure S3). Altogether these attributes establish the robustness of the VEO-CD8 co-culture model for studies of antiviral TRM differentiation and function.

Inhibition of TGF-β signaling impairs TRM differentiation in organoids

TGF-β is a multifunctional cytokine that has been implicated in epithelial TRM differentiation in numerous tissues.[25,39,40] Our pathway analysis also showed an important role of TGF-β in programming TRM differentiation in the VEO-CD8 co-culture system (Figure 3D). Consequently, we aimed to test the source and relevance of TGF-β in the co-culture system. Cell culture supernatants from wells containing CD8 T cells alone did not show measurable TGF-β1, but wells with VEOs contained significant amounts of TGF-β1 (Figure S4A). Interestingly CD8-VEO co-culture wells had higher amounts of total TGF-β1 compared to VEOs alone, but this difference was not statistically significant (Figure S4A). To test the relevance of TGF-β signaling in the context of VEO-induced TRM differentiation, we used two separate approaches. In the first approach, we used two distinct pharmacological inhibitors that block separate aspects of TGF-b signaling. The small molecule SB431542 is a potent and selective inhibitor of TGF-β type-1 receptor kinase (ALK-5) but also affects ALK-4 and ALK-7.[41] Treatment with SB431542 is thought to inhibit signaling through the TGF-β receptor. When co-cultured CD8 T cells were treated with 10 μM SB431542 for 7 days, it led to an almost complete absence of $CD69^{+}CD103^{+}$ TRMs (Figures 7A and 7B). This treatment also led to the CD8 T cells failing to downregulate CD62L, a cardinal feature of TRMs (Figures 7A and 7C). Next, we tested another small-molecule inhibitor, CWHM-12, which specifically targets αV integrins.[42] αV integrin-mediated processing of inactive TGF-β to active TGF-β has been shown to be important for CD8 TRM formation.[43–45] VEO-CD8 co-cultures were treated with various concentrations of CWHM-12, which led to a dose-dependent reduction in the percentage of $CD69^{+}CD103^{+}$ TRMs (Figures 7D and 7E). However, another property of epithelial TRMs, i.e., downregulation of Ly6C expression, was not altered in CWHM-12-treated cells (Figures 7D and 7E). Altogether our results suggested that *in vitro* FRT TRM differentiation could be prevented by pharmacological inhibition of TGF-β pathways.

To further substantiate the role of TGF-β signaling in the FRT TRM differentiation process, we used a genetic approach. We used a previously described genetic model system where dLck-Cre mice were crossed to *Tgfbr2*^{flox} mice, permitting conditional depletion of TGFbRII expression in mature T cells. Transgenic P14 CD8 T cells from TGF-βRII conditional KO donors and their wild-type (WT) counterparts were enriched and

activated *in vitro* before being introduced to the VEO-CD8 co-culture system at a 1:1 ratio. Twelve days after the co-culture, we performed phenotypic analysis of the resulting T cell population by flow cytometry. As shown in Figure 7F, among all the antigen-specific CD8 T cells (H2-Db:gp33 tetramer positive) present, the KO CD8 T cells were present at an approximately 4-fold lower rate than their WT counterparts. The KO CD8 T cells also failed to upregulate CD103 (Figures 7F and 7G). The lack of TGF-β receptor signaling also impaired CD8 T cells' ability to downregulate Ly6C and upregulate P2rx7, the latter of which is a known TGF-β-regulated gene in TRMs.[46] We next tested if TGF-β alone can mediate TRM differentiation in the absence of VEOs. However, activated CD8 T cells in suspension that were exposed to TGF-β1 failed to acquire robust TRM phenotypes compared to the VEO-co-cultured CD8 T cells (Figures S4B and S4C). This suggests that VEOs might provide other necessary signals that synergize with TGF-β to induce optimal TRM differentiation. Altogether these data support a crucial role of TGF-β signaling in mediating TRM differentiation in the VEO system.

DISCUSSION

Mice have long been the model of choice in fundamental TRM studies and have contributed immensely to our understanding of TRM biology. However, several issues with the *in vivo* model have restrained progress in generating a comprehensive picture of TRM differentiation. Chief among these is the highly inefficient extraction of TRMs from tissues via enzymatic digestion.[38] Moreover, there was bias in the extraction of cells bearing different phenotypes, e.g., $CD103^+$ TRMs were extracted more easily than the $CD103^-$ TRMs.[38] Recent work has also suggested that the routine enzymatic digestion processes can alter the transcriptome of isolated cells, potentially leading to confounding results.[47] TRMs are also highly susceptible to cell death upon isolation, complicating phenotypes and outcomes.[48,49] Lastly, separating the tissue-specific signals responsible for local TRM differentiation from systemic signals that impact other linked processes like initial T cell activation, migration, and entry into NLT is difficult in mouse models. Here, we sought to address these limitations by establishing a robust *in vitro* system for modeling TRM differentiation with epithelial organoids that solely focuses on local TRM differentiation under the influence of inductive cues produced by NLTs.

Despite its reductionist nature, the VEO system faithfully recapitulates the stratified squamous epithelium of the *in vivo* vaginal tissue, which is made up of basal, suprabasal, and cornified apical epithelium. Our co-culture system exposes CD8 T cells to products of each of these distinct epithelial cell types, which is hard to model in classical immortalized vaginal epithelial cell lines. Furthermore, the VEO co-culture model enables the detailed characterization of events specifically occurring at the final site of TRM residence, circumventing confounding factors present in live animal studies, such as the impact of CD8 T cell entry into NLT stroma. It is noteworthy that our model, while not incorporating the vaginal microbiome, offers a platform amenable to introducing bacterial species or their metabolites, enabling a detailed examination of a tripartite interaction involving epithelium-commensal microbiome-immune cells. There is a significant gap in our understanding of the impact of the vaginal microbiome on adaptive immunity, and our system could be used to fill this need.

Previous work has implicated cytokines TGF-β, IL-33, and TNF-α as crucial modulators of CD8 TRM differentiation,[8,13,23] and our study also suggested that activated CD8 T cells can differentiate into TRMs by soluble factors in the absence of physical interactions with epithelial cells. However, we failed to recapitulate this soluble-factor-mediated CD8 TRM differentiation by the simple addition of the CMs to CD8 T cells that were embedded in BME matrix. This might suggest that the pro-TRM signals have a limited half-life or became denatured during the freezing process of CMs. Characterizing the composition of the media in the co-cultured wells will enable a better understanding of the differentiation process. Another interesting finding from our co-culture studies is the pivotal role of a second antigenic exposure in further enhancing the TRM phenotype. This is in agreement with past studies that have shown the enhancement of CD8 T cell effector response as well as improvement in TRM density with second antigenic exposure.[32,33,50,51] Altogether this suggests that while cell-cell interaction might not be essential, it greatly improves epithelial TRM density. The *in vitro* VEO model also mediated the differentiation of circulating memory CD8 T cells (both TCMs and TEMs) to TRMs. However, this differentiation required antigenic reactivation of TCMs and TEMs, as has been shown *in vivo*.[38] Conversely, several recent studies have shown that mucosal, visceral, and skin TRMs can differentiate into TCMs and TEMs.[3–5,52] Because of the complexity of the *in vivo* biology and the rarity of these ex-TRMs, the cellular cues and molecular mechanisms behind this differentiation process are not well understood. We posit that the VEO-CD8 TRM model could be interrogated to understand the mechanistic basis of this dedifferentiation process.

We showed that VEOs support HSV-1 and HSV-2 replication, and as such, this model could be easily adopted for high-throughput screening of drugs or cell-based therapies that will target viral infections of the lower FRT. CD8 T cells in the co-culture model could also be genetically modified using short hairpin RNA or CRISPR to delineate the molecular underpinning of TRM development. We provided a proof-of-principle experiment showing the relevance of Runx3 in FRT TRM development, but this could easily extend to libraries of transcription factors and epigenetic modifiers implicated in T cell biology. Our co-culture approach could also be easily adopted to study human FRT TRM differentiation under the influence of local reproductive mucosa. Both ecto- and endocervical organoids have been established from human tissues recently.[53,54] The addition of T cells to these organoid cultures will improve our understanding of T cells' protective role in various diseases in a highly clinically relevant setting. Beyond the scientific advancements, our organoid model aligns with ethical considerations in animal research, adhering to the principles of replacement and reduction outlined by Russell and Burch in 1958.[55] By offering an ethically sound alternative to live animal studies, our model not only replaces the need for animal studies with a cell culture approach but also reduces the number of animals required for experimentation.

In summary, our *in vitro* TRM generation system shows that type II mucosa-derived signals are sufficient for TRM differentiation and that TGF-β is important in this differentiation process. On a broader scale, this approach presents a valuable tool for future exploration into mechanisms that govern immune defense against sexually transmitted infections and other pathogens affecting the FRT.

Limitations of the study

While our study emphasizes a critical role of epithelium-derived signals in CD8 TRM differentiation, most TRMs also collaborate with other immune cells; stromal cells, including fibroblasts; neurons; and blood vessels for their existence and function. The VEO-CD8 co-culture system does not incorporate these other tissue-derived signals. Similarly, the local commensal microbiome is a well-recognized modulator of immune cell function, and this was not included in our study. This study also utilized monoclonal TCR transgenic CD8 T cells and, as such, will not capture the TRM differentiation potential of a polyclonal repertoire with a broader range of TCR specificity and affinity. Another limitation of our work is the static nature of the cell culture platforms used to support organoid growth. *In vivo*, these structures are continuously perfused, allowing for nutrient and gas exchange as well as waste removal processes that could impact cellular differentiation, proliferation, and interactions. Future work should involve the development of complex organoid systems that incorporate other relevant cellular populations and microbial components as well as dynamic perfusion to more accurately model *in vivo* biological processes.

STAR★METHODS

RESOURCE AVAILABILITY

Lead contact—Further information and requests for resources and reagents should be directed to and will be fulfilled by Lalit K. Beura (lalit_beura@brown.edu).

Materials availability—Organoids generated in this study are available upon request.

Data and code availability

- Bulk RNA-seq data has been deposited with NCBI GEO and are publicly available as of the date of publication. Accession numbers are listed in the key resources table.
- This paper does not report original code.
- Any additional information required to reanalyze the data reported in this paper is available from the lead contact upon request.

EXPERIMENTAL MODEL AND STUDY PARTICIPANT DETAILS

Mice and infection—C57BL/6j (B6) (strain-000664), CD45.1 mice (strain-033076), CD90.1 mice (strain-000406), and OT-I CD8 T cell transgenic mice (strain-003831) were procured from the Jackson Laboratory and housed at Brown University, Providence, RI. P14 and gBT-I CD8 T cell transgenic mice were kind gifts from David Masopust (University of Minnesota) and Gregoire Lauvau (Albert Einstein College of Medicine) respectively. Congenically marked P14, gBT-I, and OT-I genotype mice were generated through crossbreeding original transgenic lines with congenic marker bearing mice strains. The *Tgfbr2*$^{f/f}$ dLck-cre+ and *Tgfbr2*$^{f/f}$ dLck-cre− P14 mice have been described before and were maintained at the animal facility at University of Texas Health at San Antonio (San Antonio, TX). Mice aged between 6 and 20 weeks were utilized in all experiments, adhering to the guidelines set forth by Brown University's or University of Texas

Health Science Center at San Antonio's Institutional Animal Care and Use Committee guidelines. Lymphocytic choriomeningitis virus (LCMV)-Armstrong was intravaginally or intraperitoneally administered using 10 μL or 200 μL of sterile RPMI-1460 media containing 2×10^5 plaque-forming units (PFU), respectively. For HSV-2 infections in mice, we used 1×10^5 PFU of HSV-2 186 kpn (TK−) per mouse. For intravaginal infections, Depo-provera (3 mg/mouse diluted with sterile PBS) was given subcutaneously 5 days before viral delivery to improve infection efficiency.

Chemicals, cytokines and peptides

Most chemicals for organoid cultures (EGF, Y-27632 (ROCK inhibitor), and SB-431542) were obtained from Sigma Aldrich. The αV integrin inhibitor, CWHM-12, was synthesized at Washington University, St. Louis and obtained via a collaboration with Peter Ruminski. Recombinant interleukin-2, 12 were purchased from Biolegend. Peptides were synthesized by Genescript or Alan Scientific to at least 95% purity.

METHOD DETAILS

Establishment of VEO-CD8 co-culture model—For establishing epithelial organoids from murine vaginal tissues, we followed a recently described protocol by Ali et al.[19] Briefly, female B6 mice aged at least 8 weeks were euthanized, and vaginal epithelium was separated from underlying stroma after overnight digestion with pronase and DNaseI. A single cell suspension of vaginal epithelial cells was prepared by pipetting, mixed with Cultrex Basement Membrane Extract (BME) (RnD Systems), and plated in 24 well plates with organoid culture medium (OC) containing DMEM/F12 media supplemented with the following agents: 1% Penicillin/streptomycin, 0.2 μg/mL Amphotericin B, 2% B27 Supplement, 5 μM SB431542, 100 ng/mL murine Epidermal growth factor (EGF), and 10 μM Y-27632. The Y-27632 was added for the first 4 days of culture only. Epithelial stem cells were allowed to differentiate and form circular organoids for 7–14 days at which point further subculturing was done to propagate the VEOs. For most co-culture studies, VEOs between passage number-3 and −8 were used. Spleen and lymph nodes from C57Bl/6j mice were isolated after euthanasia, and naive CD8 T cells were isolated using a magnet-based negative enrichment protocol following the manufacturer's direction (Mojosort mouse CD8 naive T cell isolation kit, Biolegend). These CD8 T cells were activated in the presence of anti-CD3ε (Biolegend), B7–1Fc (Biolegend), IL-2 (10 U/ml), and IL-12 (2.5 ng/ml) for 2 days. Afterward, the expanded CD8 T cells were transferred to a new 24 well plate and rested for 2 days with IL-2 alone (10U/ml). Then the effector CD8 T cells were mixed with epithelial cells obtained from trypsinized VEOs, and the cell mixture was resuspended in BME and plated at 8 μL per well on a 96-well plate. Following a 30-min incubation upside down at 37°C, 200 μL of T cell-OC culture medium (T/OC) (1% Penicillin/streptomycin, 0.2 μg/mL amphotericin B, 2% B27 Supplement, 2mM L-glutamine, 1% non-essential amino acids, 1% sodium pyruvate, 55 μM β-mercaptoethanol, 100 ng/mL EGF, 10 U/mL IL-2, and 10 μM Y-27632 added for the first 4 days of culture) media was added to each well. Media changes occurred every two days during the culture, ensuring careful handling to preserve T cells lodged in the plate.

Transwell experiment—Transwell experiments utilized MatTek cell culture inserts with 0.4 μm membranes. Organoids were trypsinized, quenched with 10% FBS in RPMI, and washed in T/OC media. The resulting single-cell suspension was either directly plated on the insert in 50 μL BME or combined with activated CD8 T cells before being plated in the bottom well at a density of 200,000 CD8 T cells per 50 μL BME. After a 30-min upside-down incubation at 37°C, 500 μL of T/OC media were added to each well. In the wells where VEOs and CD8 T cells were present in separate chambers, approximately 300,000 effector CD8 T cells were added to the lower chamber. Media in the bottom well was changed every two days. After incubation, T cells in the lower chamber were analyzed, unless otherwise stated.

Lymphocyte isolation and phenotyping—For lymphocyte isolation from *in vitro* cultured cells, well contents were collected and washed in PBS, and cells were used for staining. The lymphocyte isolation from secondary lymphoid organs (SLOs) and non-lymphoid tissues (NLTs) was performed as described with small modifications.[57] Lymphoid tissues were mashed using the plunger of a 3-mL syringe and filtered through 70 μm mesh before staining. Female reproductive tract tissues were chopped into small pieces and incubated with RPMI+2.5% FBS containing collagenase type-IV (Sigma, 1 mg/ml) and Dnase I (Sigma, 2 μg/ml) at 37°C with constant shaking for 45 min. After the incubation, tissues were further dissociated using a gentlemacs dissociator (Miltenyi Biotec) and filtered twice through a 70 μm mesh before staining.

Isolated lymphocytes were surface-stained with antibodies against CD8α (53–6.7), CD8β (YTS156.7.7), CD45.1 (A20), CD90.1 (OX-7), CD45.2 (104), CD62L (MEL-14), CD44 (IM7), CD69 (H1.2F3), CD103 (M290 or 2E7), Ly6C (HK1.4), CD49a (Ha31/8), PD1 (RMP1–30), P2rx7 (1F11), Epcam (G8.8), and CXCR6 (SA051D1). The following intracellular targets were also detected using anti-bodies-IFN-g (XMG1.2), TNF-α (MP6-XT22), IL-2 (JES6–5H4), Tbet (4B10), Eomes (Dan11mag), granzyme-B (QA16A02), and Ki67 (B56). The above antibodies were purchased from Biolegend, BD Biosciences, or Invitrogen. Cell viability was determined using Ghost Dye 780 (Tonbo Biosciences). For intracellular transcription factors and granzyme-B, the Tonbo Transcription factor staining buffer set was utilized. For intracellular cytokine staining after restimulation, the BD Cytofix/Cytoperm kit was used. Antigen-specific CD8 T cells were detected by staining with tetramers (gp33 tetramer for P14, SL8 tetramer for gBT-I, or SIINFEKL tetramer for OT-I) conjugated to brilliant violet-421 dye obtained from the NIH tetramer core facility. The stained samples were acquired using Aurora spectral cytometer (Cytek) and analyzed with FlowJo software (Treestar).

Confocal immunofluorescence microscopy—VEOs or co-culture systems were plated in a chambered cell culture slide with 50 μL of BME per well. T/OC or OC media (500 μL) was changed every two days. After 6–14 days, each sample was fixed (60 min at room temperature in 4% Paraformaldehyde) and blocked/permeabilized (overnight at 4°C in 5% normal donkey serum/0.5% Triton X-100/1X PBS). Samples were stained with unconjugated polyclonal rabbit anti-Ki67 (Abcam), unconjugated polyclonal rabbit anti-keratin-5 (Biolegend), Phycoerythrin -conjugated P63 antibody (Santacruz Biotech),

Phycoerythrin conjugated anti-Epcam monoclonal (G8.8, Biolegend), and Phycoerythrin conjugated anti-CD90.1 monoclonal (OX-7, Biolegend). Donkey anti-rabbit Cy3 conjugated antibody (Jackson Immunoresearch) was used as a secondary antibody. Primary antibodies were incubated at 4°C overnight, whereas secondary antibody was used at room temperature for 1–1.5h. DAPI was used to visualize the nucleus. Samples were washed with PBS between each step. Slides were mounted with ProLong Diamond Antifade (Invitrogen) before being imaged on an Olympus FV3000 Confocal Microscope. Captured images were processed in Fiji for visualization.

Cell sorting, RNA-seq and analysis—HSV-2 immune memory mice were prepared by transferring the 5X104 gBT-I naive CD8 T cells followed by HSV-2 intravaginal infection. Thirty days post-infection animals were euthanized and CD103+ FRT gBT-I CD8 TRM cells and CD62L + spleen gBT-I TCM cells were sort isolated. Similarly, $CD69^{+}$CD103+ CD8 T cells and total live CD8 T cells were sort isolated from VEO-CD8 cocultures and CD8 T cell cultures alone respectively. RNA was extracted from CD8 T cells using the RNeasy Plus Micro Kit (Qiagen), and libraries were constructed and sequenced on Illumina NovaSeq 2 × 150 bp paired-end sequencing (Novogene). Adapter sequences and low-quality sequences were trimmed from the raw sequence reads using Trimmomatic v0.36.[58] STAR v2.7.3a[59] was used to align the trimmed sequences to the mm10 mouse genome and to estimate the number of reads per gene. Gene count was normalized and differentially expressed genes (DEGs) were identified if Padj <0.05 in DESeq2 v1.38.1.[60] Enrichment pathway analysis utilized upregulated genes in co-cultured samples and was performed with ClusterProfiler v4.7.1[61] using MSigDB.[62] Previously published gene lists for core TRM and circulating signature[12] were used for Gene Set Enrichment Analysis (GSEA), and it was performed and visualized using the limma v3.54.1 The gene expression pattern of CD8 and co-cultured samples was compared to the previously published TCM and TRM signatures dataset GSE 147080[34] and visualized using pheatmap v1.0.12.

Quantitative PCR (qPCR)—VEOs were harvested at post-culture days 5, 9, and 15, followed by resuspension in 1 mL of cold 5 mM EDTA in DPBS in 1.5 mL Eppendorf tubes. Subsequently, the suspension was incubated on ice for 30 min. After incubation, samples were washed in 1 mL of cold DPBS by centrifugation at 1,000 × g for 5 min at 4°C, repeated twice. For the final wash, samples were collected at 1,200 × g for 5 min at 4°C. The resulting pellets were resuspended in 1 mL of TRI Reagent (Zymo Research) and incubated for 5 min at RT. 0.2 mL of chloroform was added to the tube, and the tube was shaken vigorously followed by 5 min incubation at RT. Subsequently, samples were centrifuged at 12,000 × g for 20 min at 4°C, and the clear upper layer was collected. To the obtained layer, 0.5 mL of isopropanol was added followed by a 10 min incubation at 4°C. Subsequently, samples were centrifuged at 12,000 × g for 15 min at 4°C, and the pellet was washed in 1 mL of cold 75% EtOH by centrifugation at 12,000 × g for 5 min at 4°C, repeated twice. The collected pellet was air-dried for 10 min and resuspended in 30 μL of nuclease-free water. TURBO DNA-free Kit (Invitrogen) was used to eliminate the remaining genomic DNA from the isolated RNA samples. cDNA was synthesized from the isolated RNA with the High-Capacity cDNA Reverse Transcription Kit (Thermo Fisher Scientific). qPCR reactions were prepared using Maxima SYBR Green/ROX qPCR Master

Mix (Thermo Fisher Scientific) with primer sets described in the key resource table and relative expression was calculated using the ΔΔCt method.

Retroviral transduction mediated Runx3 overexpression—Retroviral particles encoding Runx3-IRES-EGFP or mCherry alone were produced as described previously.[12] Briefly, Plat-E cells were seeded using high glucose DMEM (HyClone) supplemented with 10% fetal bovine serum in 6-well plates at a density of 5×10^5 cells/well 1 day before transfection. Transfections were performed using 1.5 μg plasmid DNA from pRunx3-EGFP and 1 μg pCL-Eco with TransIT-LT1 (Mirus) in Opti-MEM I Reduced-Serum Medium (Gibco). Retroviral supernatant was harvested 48 h and 72 h after transfection. For transductions, negatively enriched naive CD8 T cells from spleen and lymph nodes were activated in 6-well plates coated with 100 μg/mL goat anti-hamster IgG (H + L; Thermo Fisher Scientific), 1 μg/mL anti-CD3ε (145–2C11; Biolegend), and 1 μg/mL anti-CD28 (37.51; Invitrogen). T cells were subsequently transduced by replacing media with retroviral supernatant supplemented with 50 μM β-mercaptoethanol (Gibco) and 8 μg/mL polybrene (Millipore) followed by a 1 h spinfection centrifugation at 2,000 rpm and 37°C. One day after transduction, Runx3 and empty vector transduced cells were mixed 1:1, and 100,000 total cells were co-cultured with organoids for 5–10 days to generate TRM.

***In vitro* peptide restimulation assay—**After at least 7 days of VEO-CD8 T cell co-culture, the wells were treated with 0.2 μg/mL of cognate peptide (SIINFEKL for OT-I CD8 T cells, gp33 for P14 CD8 T cells, or SL8 for gBT-I CD8 T cells) for 4 h in a restimulation media containing 10% FBS, 1% penicillin/streptomycin, 1% L-glutamine, 1% non-essential amino acids, 1% sodium pyruvate, 0.25 μg/mL Amphotericin B, and 55μM β-mercaptoethanol in RPMI, supplemented with Brefeldin A. After 4 h at 37°C, the cells were collected, washed, and stained for phenotype assessment using the BD cytofix-cytoperm system as per manufacturer's instruction.

QUANTIFICATION AND STATISTICAL ANALYSIS

If the samples followed normal distribution, then parametric tests (unpaired two-tailed Student t-test for two groups and one-way ANOVA with Tukey multiple-comparison test for more than two groups) were used. If the samples deviated from a Gaussian distribution, nonparametric tests (Mann-Whitney U test for two groups and Kruskal-Wallis with Dunn multiple-comparison test for more than two groups) were used, unless otherwise stated in the figure legends. For paired analyses not conforming to Gaussian distribution, the Wilcoxon matched-pair signed-rank test was used. Shapiro-Wilk normality test was used to determine whether samples adhered to Gaussian distribution or not. Variances between groups were compared using an F test and found to be equal. All statistical analysis was done in Prism (GraphPad Software). p values < 0.05 were considered significant.

Supplementary Material

Refer to Web version on PubMed Central for supplementary material.

ACKNOWLEDGMENTS

Schematics were generated with BioRender.com. This work was supported by National Institutes of Health grants R01AI177704–01A1, R21AI183017–01, and 2P20GM109035; the Rhode Island Foundation; and the Searle Scholars Program (to L.K.B.). G.H. was supported by an American Association of Immunology Careers in Immunology Fellowship. F.J.M. was supported by the Brown Respiratory Research Training Program, NIH T32HL134625, and Molecular Biology, Cell Biology, and Biochemistry Graduate Program training grant T32GM136566. We would like to thank David Knipe (Harvard University), Betsy Herold (Albert Einstein College of Medicine), and Gregoire Lauvau (Albert Einstein College of Medicine) for providing the HSV-1gfp virus, HSV-2gfp virus, and gBT-I CD8 T cell transgenic mice, respectively. We would also like to thank Peter Ruminski (Washington University) for synthesizing the CWHM-12 compound. We acknowledge the NIH Tetramer Core Facility for providing all the tetramer reagents used in the study and the Brown University Flow Cytometry Core for facilitating the flow-based assays.

REFERENCES

1. Mueller SN, Gebhardt T, Carbone FR, and Heath WR (2013). Memory T cell subsets, migration patterns, and tissue residence. Annu. Rev. Immunol. 31, 137–161. 10.1146/annurev-immunol-032712-095954. [PubMed: 23215646]
2. Heeg M, and Goldrath AW (2023). Insights into phenotypic and functional CD8(+) T(RM) heterogeneity. Immunol. Rev. 316, 8–22. 10.1111/imr.13218. [PubMed: 37191051]
3. Fonseca R, Beura LK, Quarnstrom CF, Ghoneim HE, Fan Y, Zebley CC, Scott MC, Fares-Frederickson NJ, Wijeyesinghe S, Thompson EA, et al. (2020). Developmental plasticity allows outside-in immune responses by resident memory T cells. Nat. Immunol. 21, 412–421. 10.1038/s41590-020-0607-7. [PubMed: 32066954]
4. Christo SN, Evrard M, Park SL, Gandolfo LC, Burn TN, Fonseca R, Newman DM, Alexandre YO, Collins N, Zamudio NM, et al. (2021). Discrete tissue microenvironments instruct diversity in resident memory T cell function and plasticity. Nat. Immunol. 22, 1140–1151. 10.1038/s41590-021-01004-1. [PubMed: 34426691]
5. Behr FM, Parga-Vidal L, Kragten NAM, van Dam TJP, Wesselink TH, Sheridan BS, Arens R, van Lier RAW, Stark R, and van Gisbergen KPJM (2020). Tissue-resident memory CD8(+) T cells shape local and systemic secondary T cell responses. Nat. Immunol. 21, 1070–1081. 10.1038/s41590-020-0723-4. [PubMed: 32661361]
6. Rosato PC, Beura LK, and Masopust D (2017). Tissue resident memory T cells and viral immunity. Curr. Opin. Virol. 22, 44–50. 10.1016/j.coviro.2016.11.011. [PubMed: 27987416]
7. Paik DH, and Farber DL (2021). Anti-viral protective capacity of tissue resident memory T cells. Curr. Opin. Virol. 46, 20–26. 10.1016/j.coviro.2020.09.006. [PubMed: 33130326]
8. Slutter B, Van Braeckel-Budimir N, Abboud G, Varga SM, Salek-Ardakani S, and Harty JT (2017). Dynamics of influenza-induced lung-resident memory T cells underlie waning heterosubtypic immunity. Sci Immunol 2. 10.1126/sciimmunol.aag2031.
9. Bergsbaken T, and Bevan MJ (2015). Proinflammatory microenvironments within the intestine regulate the differentiation of tissue-resident CD8(+) T cells responding to infection. Nat. Immunol. 16, 406–414. 10.1038/ni.3108. [PubMed: 25706747]
10. Iijima N, and Iwasaki A (2014). T cell memory. A local macrophage chemokine network sustains protective tissue-resident memory CD4 T cells. Science 346, 93–98. 10.1126/science.1257530. [PubMed: 25170048]
11. Mackay LK, Minnich M, Kragten NAM, Liao Y, Nota B, Seillet C, Zaid A, Man K, Preston S, Freestone D, et al. (2016). Hobit and Blimp1 instruct a universal transcriptional program of tissue residency in lymphocytes. Science 352, 459–463. 10.1126/science.aad2035. [PubMed: 27102484]
12. Milner JJ, Toma C, Yu B, Zhang K, Omilusik K, Phan AT, Wang D, Getzler AJ, Nguyen T, Crotty S, et al. (2017). Runx3 programs CD8(+) T cell residency in non-lymphoid tissues and tumours. Nature 552, 253–257. 10.1038/nature24993. [PubMed: 29211713]
13. Skon CN, Lee JY, Anderson KG, Masopust D, Hogquist KA, and Jameson SC (2013). Transcriptional downregulation of S1pr1 is required for the establishment of resident memory CD8+ T cells. Nat. Immunol. 14, 1285–1293. 10.1038/ni.2745. [PubMed: 24162775]

14. Bar-Ephraim YE, Kretzschmar K, and Clevers H (2020). Organoids in immunological research. Nat. Rev. Immunol. 20, 279–293. 10.1038/s41577-019-0248-y. [PubMed: 31853049]
15. Blutt SE, and Estes MK (2022). Organoid Models for Infectious Disease. Annu. Rev. Med. 73, 167–182. 10.1146/annurev-med-042320-023055. [PubMed: 34644153]
16. Kim J, Koo BK, and Knoblich JA (2020). Human organoids: model systems for human biology and medicine. Nat. Rev. Mol. Cell Biol. 21, 571–584. 10.1038/s41580-020-0259-3. [PubMed: 32636524]
17. Xu H, Lyu X, Yi M, Zhao W, Song Y, and Wu K (2018). Organoid technology and applications in cancer research. J. Hematol. Oncol. 11, 116. 10.1186/s13045-018-0662-9. [PubMed: 30219074]
18. Ali A, Syed SM, Jamaluddin MFB, Colino-Sanguino Y, Gallego-Ortega D, and Tanwar PS (2020). Cell Lineage Tracing Identifies Hormone-Regulated and Wnt-Responsive Vaginal Epithelial Stem Cells. Cell Rep. 30, 1463–1477.e7. 10.1016/j.celrep.2020.01.003. [PubMed: 32023462]
19. Ali A, Syed SM, and Tanwar PS (2020). Protocol for In Vitro Establishment and Long-Term Culture of Mouse Vaginal Organoids. STAR Protoc. 1, 100088. 10.1016/j.xpro.2020.100088. [PubMed: 33111121]
20. Cooley A, Madhukaran S, Stroebele E, Colon Caraballo M, Wang L, Akgul Y, Hon GC, and Mahendroo M (2023). Dynamic states of cervical epithelia during pregnancy and epithelial barrier disruption. iScience 26, 105953. 10.1016/j.isci.2023.105953. [PubMed: 36718364]
21. Houghton O, and McCluggage WG (2009). The expression and diagnostic utility of p63 in the female genital tract. Adv. Anat. Pathol. 16, 316–321. 10.1097/PAP.0b013e3181b507c6. [PubMed: 19700941]
22. Tucker CG, Mitchell JS, Martinov T, Burbach BJ, Beura LK, Wilson JC, Dwyer AJ, Singh LM, Mescher MF, and Fife BT (2020). Adoptive T Cell Therapy with IL-12-Preconditioned Low-Avidity T Cells Prevents Exhaustion and Results in Enhanced T Cell Activation, Enhanced Tumor Clearance, and Decreased Risk for Autoimmunity. J. Immunol. 205, 1449–1460. 10.4049/jimmunol.2000007. [PubMed: 32737148]
23. Casey KA, Fraser KA, Schenkel JM, Moran A, Abt MC, Beura LK, Lucas PJ, Artis D, Wherry EJ, Hogquist K, et al. (2012). Antigen-independent differentiation and maintenance of effector-like resident memory T cells in tissues. J. Immunol. 188, 4866–4875. 10.4049/jimmunol.1200402. [PubMed: 22504644]
24. Sheridan BS, Pham QM, Lee YT, Cauley LS, Puddington L, and Lefranç ois L (2014). Oral infection drives a distinct population of intestinal resident memory CD8(+) T cells with enhanced protective function. Immunity 40, 747–757. 10.1016/j.immuni.2014.03.007. [PubMed: 24792910]
25. Mackay LK, Rahimpour A, Ma JZ, Collins N, Stock AT, Hafon ML, Vega-Ramos J, Lauzurica P, Mueller SN, Stefanovic T, et al. (2013). The developmental pathway for CD103(+)CD8+ tissue-resident memory T cells of skin. Nat. Immunol. 14, 1294–1301. 10.1038/ni.2744. [PubMed: 24162776]
26. Beura LK, Mitchell JS, Thompson EA, Schenkel JM, Mohammed J, Wijeyesinghe S, Fonseca R, Burbach BJ, Hickman HD, Vezys V, et al. (2018). Intravital mucosal imaging of CD8(+) resident memory T cells shows tissue-autonomous recall responses that amplify secondary memory. Nat. Immunol. 19, 173–182. 10.1038/s41590-017-0029-3. [PubMed: 29311694]
27. Dave VA, Cardozo-Ojeda EF, Mair F, Erickson J, Woodward-Davis AS, Koehne A, Soerens A, Czartoski J, Teague C, Potchen N, et al. (2021). Cervicovaginal Tissue Residence Confers a Distinct Differentiation Program upon Memory CD8 T Cells. J. Immunol. 206, 2937–2948. 10.4049/jimmunol.2100166. [PubMed: 34088770]
28. Kumar BV, Ma W, Miron M, Granot T, Guyer RS, Carpenter DJ, Senda T, Sun X, Ho SH, Lerner H, et al. (2017). Human Tissue-Resident Memory T Cells Are Defined by Core Transcriptional and Functional Signatures in Lymphoid and Mucosal Sites. Cell Rep. 20, 2921–2934. 10.1016/j.celrep.2017.08.078. [PubMed: 28930685]
29. Bromley SK, Akbaba H, Mani V, Mora-Buch R, Chasse AY, Sama A, and Luster AD (2020). CD49a Regulates Cutaneous Resident Memory CD8(+) T Cell Persistence and Response. Cell Rep. 32, 108085. 10.1016/j.celrep.2020.108085. [PubMed: 32877667]
30. Reilly EC, Lambert Emo K, Buckley PM, Reilly NS, Smith I, Chaves FA, Yang H, Oakes PW, and Topham DJ (2020). T(RM) integrins CD103 and CD49a differentially support adherence

and motility after resolution of influenza virus infection. Proc. Natl. Acad. Sci. USA 117, 12306–12314. 10.1073/pnas.1915681117. [PubMed: 32439709]

31. Mackay LK, Wynne-Jones E, Freestone D, Pellicci DG, Mielke LA, Newman DM, Braun A, Masson F, Kallies A, Belz GT, and Carbone FR (2015). T-box Transcription Factors Combine with the Cytokines TGF-beta and IL-15 to Control Tissue-Resident Memory T Cell Fate. Immunity 43, 1101–1111. 10.1016/j.immuni.2015.11.008. [PubMed: 26682984]
32. Khan TN, Mooster JL, Kilgore AM, Osborn JF, and Nolz JC (2016). Local antigen in nonlymphoid tissue promotes resident memory CD8+ T cell formation during viral infection. J. Exp. Med. 213, 951–966. 10.1084/jem.20151855. [PubMed: 27217536]
33. McMaster SR, Wein AN, Dunbar PR, Hayward SL, Cartwright EK, Denning TL, and Kohlmeier JE (2018). Pulmonary antigen encounter regulates the establishment of tissue-resident CD8 memory T cells in the lung airways and parenchyma. Mucosal Immunol. 11, 1071–1078. 10.1038/s41385-018-0003-x. [PubMed: 29453412]
34. Milner JJ, Toma C, He Z, Kurd NS, Nguyen QP, McDonald B, Quezada L, Widjaja CE, Witherden DA, Crowl JT, et al. (2020). Heterogenous Populations of Tissue-Resident CD8(+) T Cells Are Generated in Response to Infection and Malignancy. Immunity 52, 808–824.e7. 10.1016/j.immuni.2020.04.007. [PubMed: 32433949]
35. Qiu Z, Khairallah C, Chu TH, Imperato JN, Lei X, Romanov G, Ata-kilit A, Puddington L, and Sheridan BS (2023). Retinoic acid signaling during priming licenses intestinal CD103+ CD8 TRM cell differentiation. J. Exp. Med. 220, e20210923. 10.1084/jem.20210923. [PubMed: 36809399]
36. Desai P, and Person S (1998). Incorporation of the green fluorescent protein into the herpes simplex virus type 1 capsid. J. Virol. 72, 7563–7568. 10.1128/JVI.72.9.7563-7568.1998. [PubMed: 9696854]
37. Cheshenko N, Trepanier JB, González PA, Eugenin EA, Jacobs WR Jr., and Herold BC (2014). Herpes simplex virus type 2 glycoprotein H interacts with integrin alphavbeta3 to facilitate viral entry and calcium signaling in human genital tract epithelial cells. J. Virol. 88, 10026–10038. 10.1128/JVI.00725-14. [PubMed: 24942591]
38. Steinert EM, Schenkel JM, Fraser KA, Beura LK, Manlove LS, Igyártó BZ, Southern PJ, and Masopust D (2015). Quantifying Memory CD8 T Cells Reveals Regionalization of Immunosurveillance. Cell 161, 737–749. 10.1016/j.cell.2015.03.031. [PubMed: 25957682]
39. Goplen NP, Wu Y, Son YM, Li C, Wang Z, Cheon IS, Jiang L, Zhu B, Ayasoufi K, Chini EN, et al. (2020). Tissue-resident CD8(+) T cells drive age-associated chronic lung sequelae after viral pneumonia. Sci. Immunol. 5, eabc4557. 10.1126/sciimmunol.abc4557. [PubMed: 33158975]
40. Zhang N, and Bevan MJ (2013). Transforming growth factor-beta signaling controls the formation and maintenance of gut-resident memory T cells by regulating migration and retention. Immunity 39, 687–696. 10.1016/j.immuni.2013.08.019. [PubMed: 24076049]
41. Inman GJ, Nicolás FJ, Callahan JF, Harling JD, Gaster LM, Reith AD, Laping NJ, and Hill CS (2002). SB-431542 is a potent and specific inhibitor of transforming growth factor-beta superfamily type I activin receptor-like kinase (ALK) receptors ALK4, ALK5, and ALK7. Mol. Pharmacol. 62, 65–74. 10.1124/mol.62.1.65. [PubMed: 12065756]
42. Henderson NC, Arnold TD, Katamura Y, Giacomini MM, Rodriguez JD, McCarty JH, Pellicoro A, Raschperger E, Betsholtz C, Ruminski PG, et al. (2013). Targeting of alphav integrin identifies a core molecular pathway that regulates fibrosis in several organs. Nat. Med. 19, 1617–1624. 10.1038/nm.3282. [PubMed: 24216753]
43. Hirai T, Yang Y, Zenke Y, Li H, Chaudhri VK, De La Cruz Diaz JS, Zhou PY, Nguyen BA, Bartholin L, Workman CJ, et al. (2021). Competition for Active TGFbeta Cytokine Allows for Selective Retention of Antigen-Specific Tissue-Resident Memory T Cells in the Epidermal Niche. Immunity 54, 84–98.e85. 10.1016/j.immuni.2020.10.022. [PubMed: 33212014]
44. Mohammed J, Beura LK, Bobr A, Astry B, Chicoine B, Kashem SW, Welty NE, Igyárto BZ, Wijeyesinghe S, Thompson EA, et al. (2016). Stromal cells control the epithelial residence of DCs and memory T cells by regulated activation of TGF-beta. Nat. Immunol. 17, 414–421. 10.1038/ni.3396. [PubMed: 26901152]
45. Ferreira C, Barros L, Baptista M, Blankenhaus B, Barros A, Figueir-edo-Campos P, Konjar Š, Laine A, Kamenjarin N, Stojanovic A, et al. (2020). Type 1 T(reg) cells promote the generation of

CD8(+) tissue-resident memory T cells. Nat. Immunol. 21, 766–776. 10.1038/s41590-020-0674-9. [PubMed: 32424367]

46. Borges da Silva H, Peng C, Wang H, Wanhainen KM, Ma C, Lopez S, Khoruts A, Zhang N, and Jameson SC (2020). Sensing of ATP via the Purinergic Receptor P2RX7 Promotes CD8(+) Trm Cell Generation by Enhancing Their Sensitivity to the Cytokine TGF-beta. Immunity 53, 158–171.e156. 10.1016/j.immuni.2020.06.010. [PubMed: 32640257]
47. Crowl JT, Heeg M, Ferry A, Milner JJ, Omilusik KD, Toma C, He Z, Chang JT, and Goldrath AW (2022). Tissue-resident memory CD8(+) T cells possess unique transcriptional, epigenetic and functional adaptations to different tissue environments. Nat. Immunol. 23, 1121–1131. 10.1038/s41590-022-01229-8. [PubMed: 35761084]
48. Kunzli M, Schreiner D, Pereboom TC, Swarnalekha N, Litzler LC, Lötscher J, Ertuna YI, Roux J, Geier F, Jakob RP, et al. (2020). Long-lived T follicular helper cells retain plasticity and help sustain humoral immunity. Sci. Immunol. 5. 10.1126/sciimmunol.aay5552.
49. Borges da Silva H, Wang H, Qian LJ, Hogquist KA, and Jameson SC (2019). ARTC2.2/P2RX7 Signaling during Cell Isolation Distorts Function and Quantification of Tissue-Resident CD8(+) T Cell and Invariant NKT Subsets. J. Immunol. 202, 2153–2163. 10.4049/jimmunol.1801613. [PubMed: 30777922]
50. Jiang X, Clark RA, Liu L, Wagers AJ, Fuhlbrigge RC, and Kupper TS (2012). Skin infection generates non-migratory memory CD8+ T(RM) cells providing global skin immunity. Nature 483, 227–231. 10.1038/nature10851. [PubMed: 22388819]
51. McKinstry KK, Strutt TM, Bautista B, Zhang W, Kuang Y, Cooper AM, and Swain SL (2014). Effector CD4 T-cell transition to memory requires late cognate interactions that induce autocrine IL-2. Nat. Commun. 5, 5377. 10.1038/ncomms6377. [PubMed: 25369785]
`52. Klicznik MM, Morawski PA, Höllbacher B, Varkhande SR, Motley SJ, Kuri-Cervantes L, Goodwin E, Rosenblum MD, Long SA, Brachtl G, et al. (2019). Human CD4(+)CD103(+) cutaneous resident memory T cells are found in the circulation of healthy individuals. Sci. Immunol. 4, eaav8995. 10.1126/sciimmunol.aav8995. [PubMed: 31278120]
53. Lohmussaar K, Oka R, Espejo Valle-Inclan J, Smits MHH, Wardak H, Korving J, Begthel H, Proost N, van de Ven M, Kranenburg OW, et al. (2021). Patient-derived organoids model cervical tissue dynamics and viral oncogenesis in cervical cancer. Cell Stem Cell 28, 1380–1396.e1386. 10.1016/j.stem.2021.03.012. [PubMed: 33852917]
54. Gurumurthy RK, Koster S, Kumar N, Meyer TF, and Chumduri C (2022). Patient-derived and mouse endo-ectocervical organoid generation, genetic manipulation and applications to model infection. Nat. Protoc. 17, 1658–1690. 10.1038/s41596-022-00695-6. [PubMed: 35546639]
55. Tannenbaum J, and Bennett BT (2015). Russell and Burch's 3Rs then and now: the need for clarity in definition and purpose. J. Am. Assoc. Lab. Anim. Sci. 54, 120–132. [PubMed: 25836957]
56. Mueller SN, Heath W, McLain JD, Carbone FR, and Jones CM (2002). Characterization of two TCR transgenic mouse lines specific for herpes simplex virus. Immunol. Cell Biol. 80, 156–163. 10.1046/j.1440-1711.2002.01071.x. [PubMed: 11940116]
57. Beura LK, Scott MC, Pierson MJ, Joag V, Wijeyesinghe S, Semler MR, Quarnstrom CF, Busman-Sahay K, Estes JD, Hamilton SE, et al. (2022). Novel Lymphocytic Choriomeningitis Virus Strain Sustains Abundant Exhausted Progenitor CD8 T Cells without Systemic Viremia. J. Immunol. 209, 1691–1702. 10.4049/jimmunol.2200320. [PubMed: 36122933]
58. Bolger AM, Lohse M, and Usadel B (2014). Trimmomatic: a flexible trimmer for Illumina sequence data. Bioinformatics 30, 2114–2120. 10.1093/bioinformatics/btu170. [PubMed: 24695404]
59. Dobin A, Davis CA, Schlesinger F, Drenkow J, Zaleski C, Jha S, Batut P, Chaisson M, and Gingeras TR (2013). STAR: ultrafast universal RNA-seq aligner. Bioinformatics 29, 15–21. 10.1093/bioinformatics/bts635. [PubMed: 23104886]
60. Love MI, Huber W, and Anders S (2014). Moderated estimation of fold change and dispersion for RNA-seq data with DESeq2. Genome Biol. 15, 550. 10.1186/s13059-014-0550-8. [PubMed: 25516281]

61. Yu G, Wang LG, Han Y, and He QY (2012). clusterProfiler: an R package for comparing biological themes among gene clusters. cluster-Profiler: an R package for comparing biological themes among gene clusters 16, 284–287. 10.1089/omi.2011.0118.

62. Castanza AS, Recla JM, Eby D, Thorvaldsdóttir H, Bult CJ, and Mesirov JP (2023). Extending support for mouse data in the Molecular Signatures Database (MSigDB). Nat. Methods 20, 1619–1620. 10.1038/s41592-023-02014-7. [PubMed: 37704782]

Highlights

- Vaginal epithelial stem cells form organoids mimicking *in vivo* vaginal epithelium
- CD8 T cells co-cultured with organoids differentiate into resident memory CD8 T cells
- *In vitro* CD8 TRMs phenotypically and transcriptionally resemble *in vivo* epithelial TRMs
- VEO-CD8 co-culture model can be interrogated to reveal fundamental TRM biology

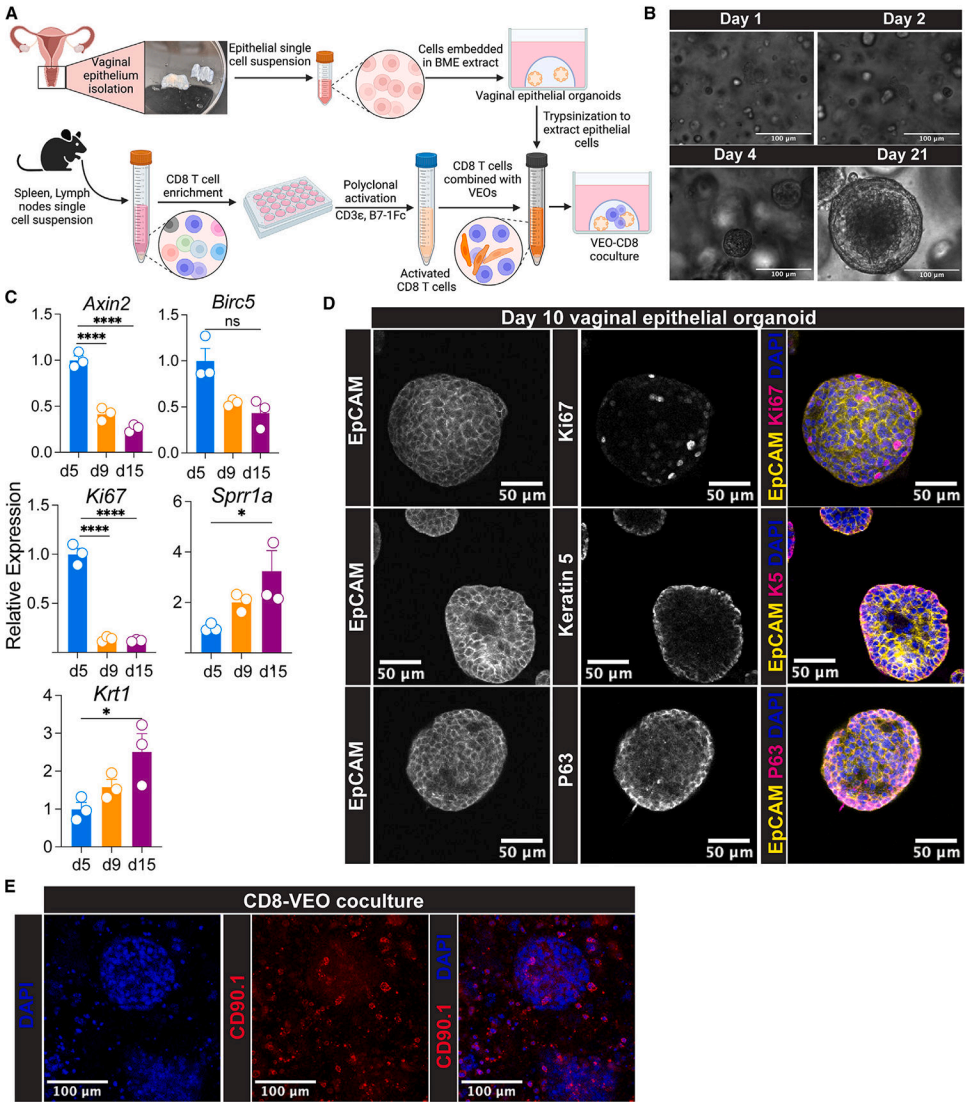

Figure 1. Establishment of VEOs and co-culturing with CD8 T lymphocytes

(A) Schematics describing differentiation of vaginal epithelial organoids (VEOs) using growth factors and chemicals. Activated CD8 T cells were co-cultured with VEOs to enable CD8 T cells' differentiation to TRMs.

(B) Representative differential interference contrast microscopy of VEOs at day 1, 2, 4, and 21 post-subculture showing growth. Scale bar: 100 µm.

(C) Relative RNA level of indicated genes detected by quantitative PCR at different days post-subculture showing differential levels of distinct epithelial populations within the VEOs as they grow.

(D) Representative confocal microscopy images of VEOs showing epithelial identity as well as different layers. Top row: Epcam, yellow; Ki67, magenta; DAPI, blue. Middle row: Epcam, yellow; keratin-5, magenta; DAPI, blue. Bottom row: Epcam, yellow; P63, magenta; DAPI, blue. Scale bar: 50 µm.

(E) Activated CD8 T cells stained with a congenic marker CD90.1 (red) were co-cultured with VEOs and a representative confocal microscopy image 7 days post-culture is shown. Scale bar: 100 μm.

Schematic in (A) was made with BioRender. Experiments in (B)–(E) were repeated at least twice with more than 3 separate wells/condition. One-way ANOVA with Tukey's multiple comparison test (C; *Axin2*, *Ki67*, *Sprr1a*, and *Krt1*). Kruskal-Wallis ANOVA with Dunn's multiple comparison test (C; *Birc5*). $*p < 0.05$, $**p < 0.01$, $***p < 0.001$, and $****p < 0.0001$.

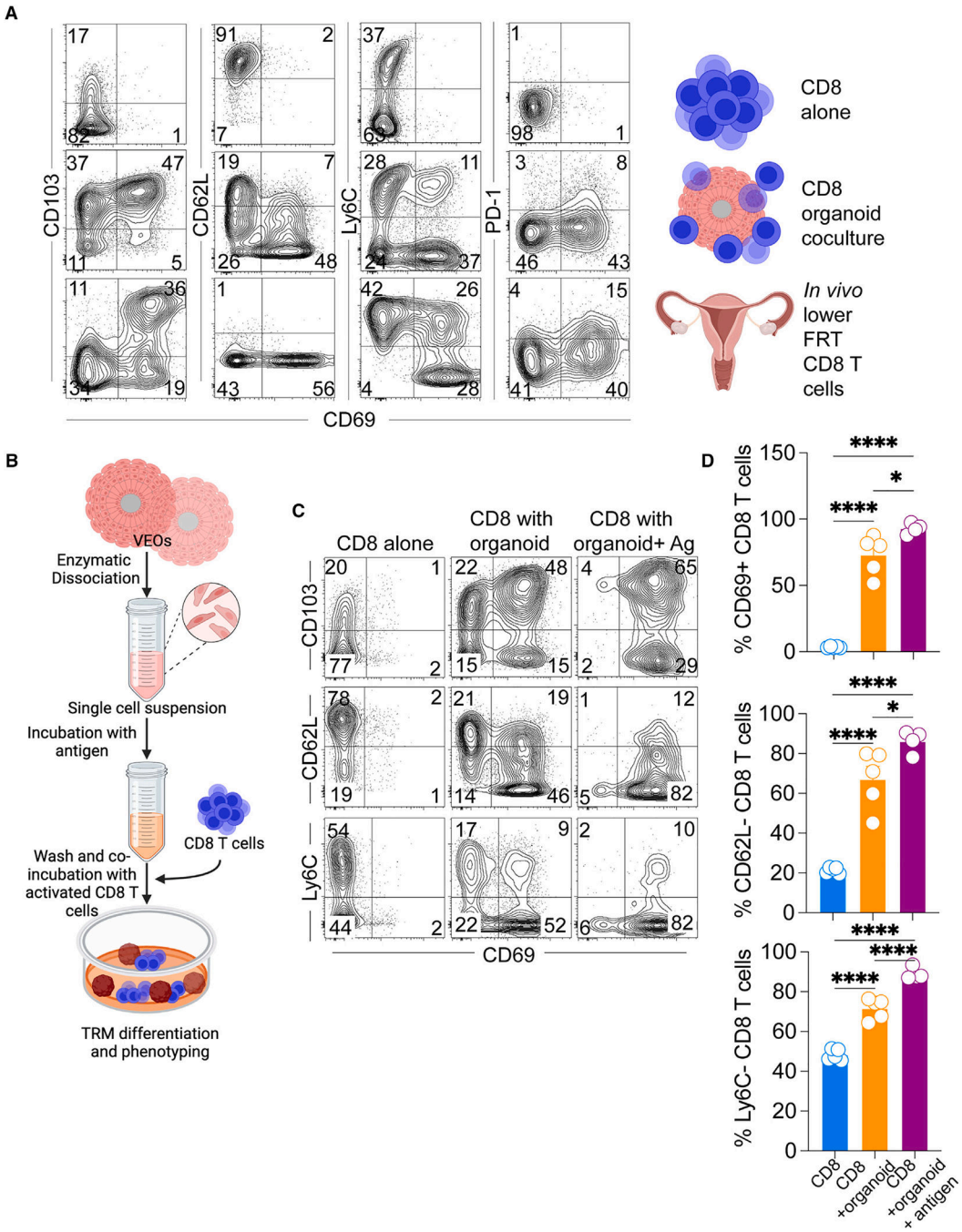

Figure 2. Co-cultured CD8 T cells adopt phenotypic characteristics of TRMs

(A) CD8 T cells maintained alone (top row) or embedded with the VEOs (middle row) were isolated at day 14 post-culture and representative flow plots depicting expression of various TRM-associated markers are shown. Both rows were gated on live congenic marker (CD45.1 or CD90.1)$^{+}$ CD8 T cells. Flow plots in the bottom row are viral antigen ($gB_{498–505}$)-specific memory CD8 T cells isolated from the lower FRT of mice infected with HSV-2 intravaginally 35 days prior. The plots are gated on live antigen-specific CD8 T cells located in the tissue parenchyma (IV negative).

(B) Schematics describing the protocol used to expose the activated CD8 T cells to cognate antigen again during the co-culture.

(C and D) Flow cytometry phenotype of CD8 T cells exposed to antigen (gp33 peptide) leading to enhanced acquisition of TRM characteristics. Representative flow plots shown in (C) are gated on live $CD45.1^+$ or $CD90.1^+$ CD8 T cells, and percentages are enumerated in (D). Bars indicate mean ± SEM. Data are representative of three repeats with $n = 4–6$/condition. One-way ANOVA with Tukey's multiple comparison test (D). *$p < 0.05$, **$p < 0.01$, ***$p < 0.001$, and ****$p < 0.0001$.

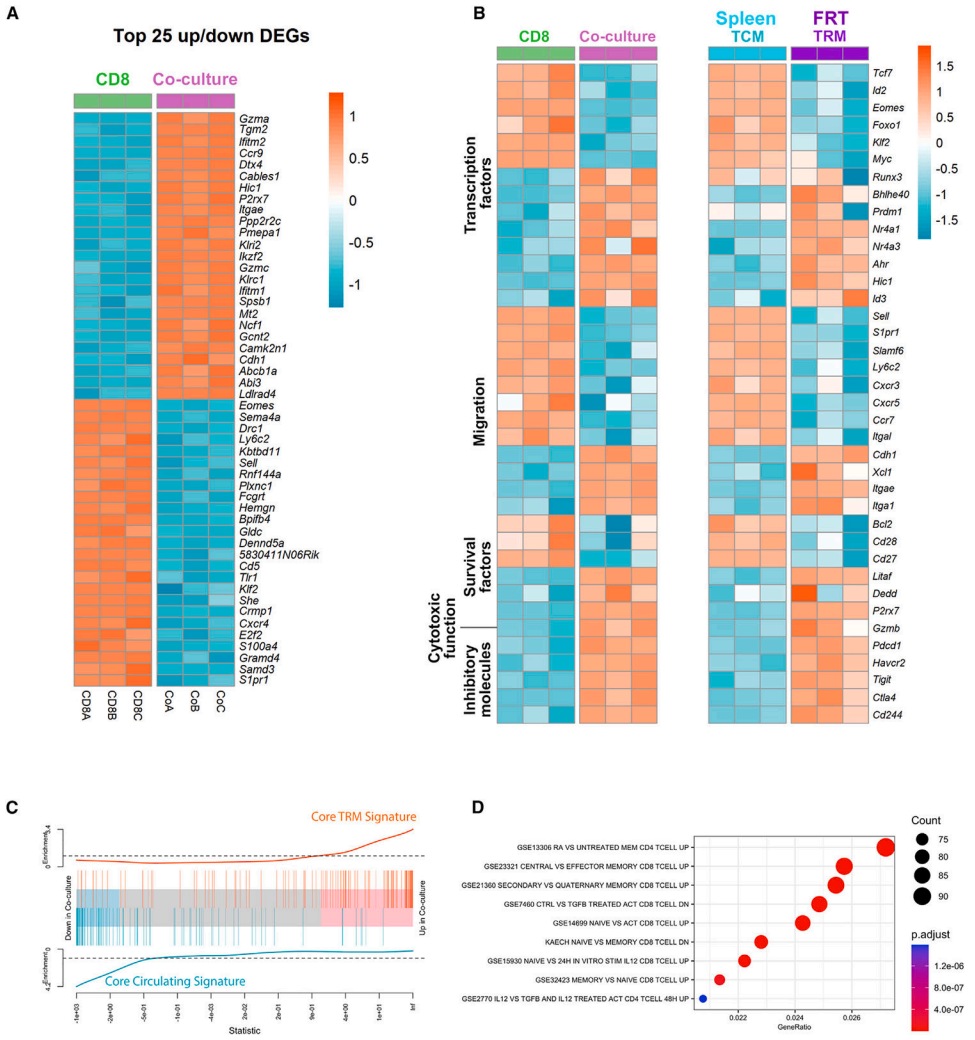

Figure 3. Transcriptional overlap between bona fide *in vivo* TRMs and *in vitro* differentiated TRMs

(A) Heatmap of top 25 differentially up-/downregulated genes between CD8 TRMs generated via co-culture with VEOs vs. CD8 T cells maintained alone. The score was calculated as −log10(*p*adj)*log2FC, and differentially expressed genes (DEGs) were based on this score. *p*adj, adjusted *p* value; log2FC, log2 fold change.

(B) Expression of selected gene sets belonging to indicated categories between CD8 and co-cultured TRMs ($CD69^{+}CD103^{+}$). Expression level of these same genes for circulating H2: Kb-$gB_{498–505}$ + CD8 TCMs and CD8 TRMs from FRT of HSV-2-infected mice.

(C) Gene set enrichment analysis (GSEA) plot. Core TRM and core circulating gene signature was created using a ranked gene list from published data comparing TRMs and TCMs (GEO: GSE147080).[12] Enrichment of the overexpressed and underexpressed *in vitro* TRM gene sets in this ranked list is plotted.

(D) Enriched pathways in *in vitro* TRMs based on MSigDB are shown.

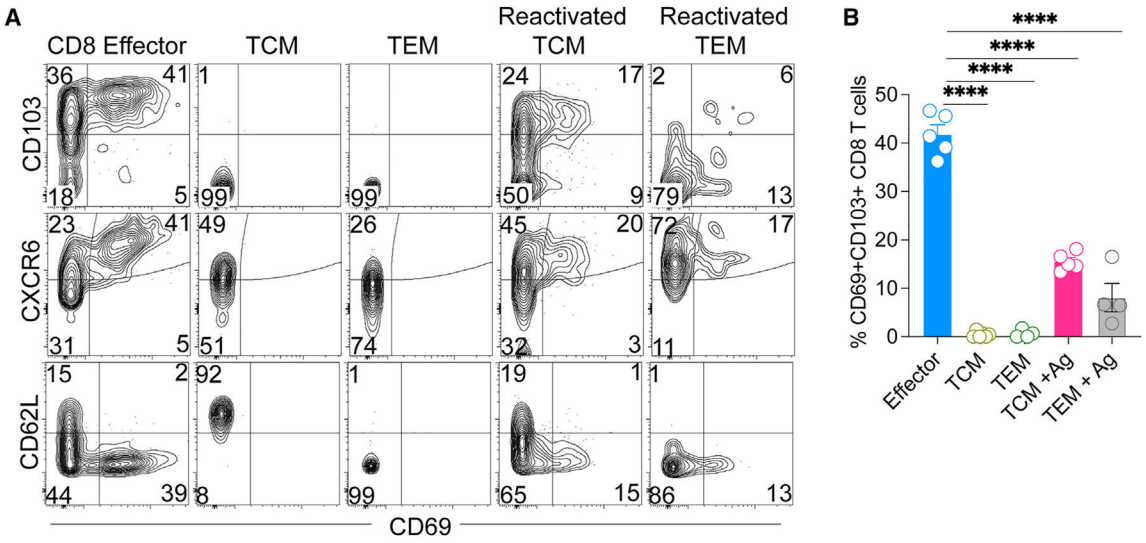

Figure 4. Circulating memory CD8 T cells need to be reactivated to form TRMs under the influence of VEOs

(A and B) C57BL/6J mice received 10^4 CD45.1$^+$ naive P14 CD8 T cells and were infected with LCMV. At 70 dpi, SLOs were harvested, and TCMs (live CD8a$^+$CD45.1$^+$CD62L$^+$) and TEMs (live CD8a$^+$CD45.1$^+$CD62L$^-$) were flow sorted and incubated with VEOs for 10 days. In some cases, the cells were exposed to epithelial cells loaded with gp33 peptide (0.2 μg/mL) labeled as reactivated cells. Naive CD8 T cells differentiated *in vitro* and co-cultured with VEOs were included as a control (effector). Representative flow plots are shown in (A), gated on live congenic marker (CD45.1) T cells, and percentages are enumerated in (B). Data are representative of two repeats with $n = 3–5$/condition. Bars indicate mean ± SEM. One-way ANOVA with Tukey's multiple comparison test (B). ****$p < 0.0001$.

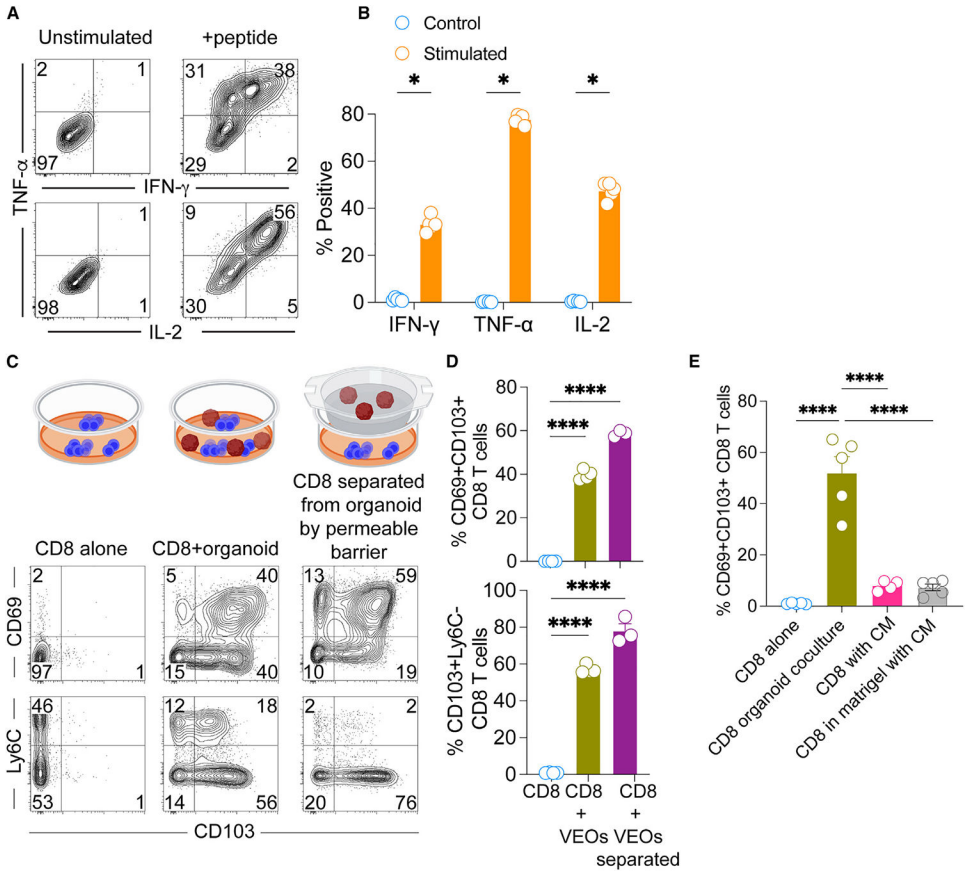

Figure 5. *In-vitro*-differentiated CD8 TRMs remain functional and could be generated in the absence of physical association with VEOs

(A) Co-cultured CD8 T cells (day 11) were stimulated with antigenic peptide or unstimulated for 4 h in the presence of brefeldin A. Representative flow plots showing expression of the cytokines interferon (IFN)-γ, TNF-α, and IL-2 are shown. Plots are gated on live CD8β$^+$ T cells.

(B) Percentage of stimulated cells expressing various cytokines are compared against unstimulated cells.

(C) Transwell assays were conducted whereby CD8 T cells in the bottom chamber were exposed to soluble mediators released from VEOs for a period of 10 days. This was compared to CD8 T cells cultured in the absence of VEOs and CD8 T cells embedded together with VEOs. Representative flow plots are gated on live CD8β $^+$ T cells showing robust adoption of the TRM phenotype when CD8 T cells were separated from VEOs by the semipermeable barrier.

(D) Bar graph showing percentage of positivity of various TRM phenotypes.

(E) Regular exposure to VEO conditioned medium (CM) for 10 days was not sufficient to drive CD69$^+$CD103$^+$ epithelial TRM phenotype. Bar graph comparing various CM treatments with the regular co-culture system is shown. Data are representative of three repeats with n = 3–6/condition (B and D) and two repeats with n = 5/condition (E). Bars indicate mean ± SEM. Multiple Student's t tests (B). One-way ANOVA with Tukey's multiple comparison test (D and E). *$p < 0.05$ and ****$p < 0.0001$.

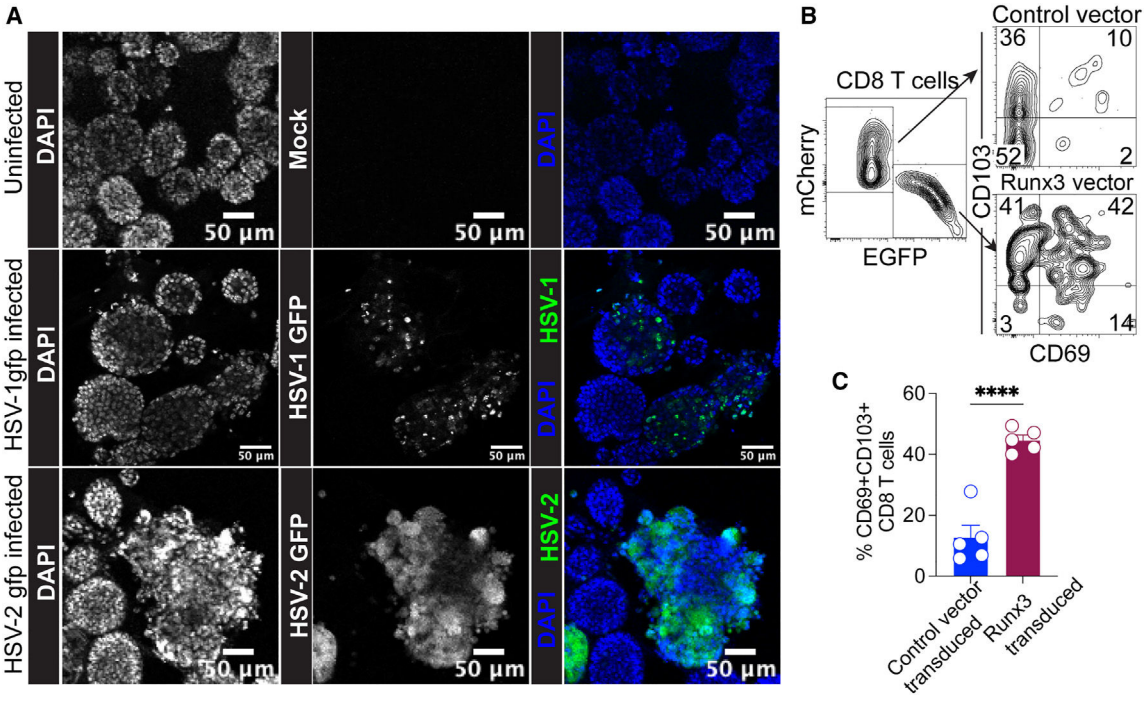

Figure 6. VEOs support viral replication, and the co-culture system is amenable to genetic perturbation

(A) 7-day-old VEOs were mock infected or infected with HSV-1 K26GFP or HSV-2(333ZAG)-GFP. Wells containing infected and uninfected cells were visualized 24 h post-infection using confocal microscopy. Representative images are shown. Scale bar: 50 µm.

(B) *In-vitro*-activated P14 CD8 T cells were retrovirally transduced with Runx3-EGFP-expressing vector or control-mCherry-expressing vector. Equivalent numbers of cells were cultured with VEOs for 10 days, and their ability to form TRMs was tested by flow cytometry. Representative flow plots of total transgene-positive P14 cells are shown on the left, and the levels of CD69 and CD103 on the two reporter-positive populations are shown on the right.

(C) Bar graph comparing percentage of $CD69^{+}CD103^{+}$ cells among the two transduced populations. Data are representative of two repeats with at least n =3 wells/condition. Bars indicate mean ± SEM. Student's t test. ****$p < 0.0001$.

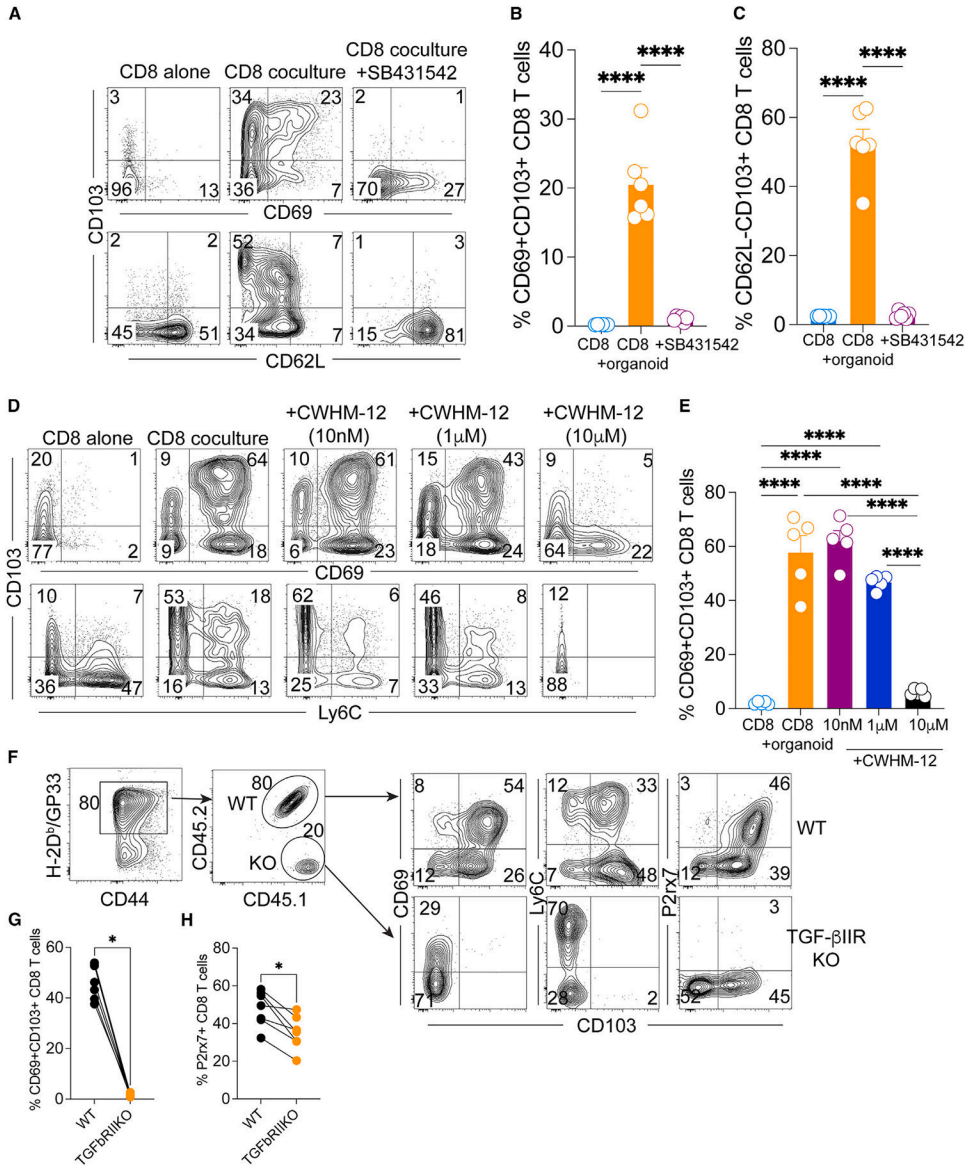

Figure 7. Pharmacological and genetic inhibition of TGF-β signaling interferes with *in vitro* TRM generation

(A) CD8 T cells co-cultured with VEOs were treated with TGF-β signaling inhibitor, SB431542 (10 μM), or vehicle control for 7 days. Representative flow plots of live CD8β$^+$ T cells are shown.

(B and C) Percentages of TRM phenotype cell are enumerated. CD8 T cells maintained alone are included as a control.

(D) CD8 T cells co-cultured with VEOs were treated with increasing concentrations of an inhibitor of TGF-β activating αV integrins, CWHM-12 (10 nM–10 μM), or vehicle for 12 days. Representative flow plots of live CD8β $^+$ T cells are shown.

(E) Percentages of CD69$^+$CD103$^+$ phenotype cells are enumerated.

(F) TGF-β-receptor-deficient CD8 T cells fail to adopt TRM phenotype in the VEO co-culture model. Wild-type (WT; CD45.1$^+$CD45.2$^+$) and TGF-βRII-deficient P14 (KO,

CD45.1^{+}CD45.2^{-}) CD8 T cells were activated and embedded in BME containing VEOs at a 1:1 ratio. Representative flow plots 12 days after the co-incubation are shown. Total P14 CD8 T cells and the ratio of WT and KO CD8 T cell percentages retained as well as their associated phenotypes after 12 days are shown.

(G and H) Comparison of CD69^{+}CD103^{+} CD8 T cells and H. p2rx7^{+} CD8 T cells between WT and KO groups. Data are representative of two repeats with n = 4–6/condition. Bars indicate mean ± SEM.

One-way ANOVA with Tukey's multiple comparison test (B, C, and E). Wilcoxon matched-pairs signed rank test (G and H). *$p < 0.05$ and ****$p < 0.0001$.

KEY RESOURCES TABLE

REAGENT or RESOURCE	SOURCE	IDENTIFIER
Antibodies		
Anti-CD62L (MEL-14)	Biolegend	Cat# 104438, RRID:AB_2563058
Anti-CD62L (MEL-14)	Biolegend	Cat# 104453, RRID: AB_2800559
Anti-CD103 (2E7)	Biolegend	Cat# 121420, RRID:AB_10714791
Anti-EpCAM (G8.8)	Biolegend	Cat# 118206, RRID: AB_1134172
Anti-CD90.1 (OX-7)	Biolegend	Cat# 202539, RRID: AB_2562645
Anti-CD90.1 (OX-7)	Biolegend	Cat# 202522, RRID: AB_1595477
Anti-CD45.1 (A20)	Biolegend	Cat# 110722, RRID: AB_492866
Anti-CD45.1 (A20)	Biolegend	Cat# 110708, RRID: AB_313497
Anti-Ly-6C (HK1.4)	Biolegend	Cat# 128041, RRID: AB_2565852
Anti-CD69 (H1.2F3)	Biolegend	Cat# 104536, RRID: AB_2565583
Anti-CD69 (H1.2F3)	Biolegend	Cat# 104507, RRID: AB_313110
Anti-CD69 (H1.2F3)	Biolegend	Cat# 104518, RRID: AB_492847
Anti-CD69 (H1.2F3)	Biolegend	Cat# 104545, RRID: AB_2686969
Anti-CD8a (53–6.7)	Biolegend	Cat# 100734, RRID: AB_2075238
Anti-CD8b (YTS156.7.7)	Biolegend	Cat# 126610, RRID: AB_2260149
Anti-CD44 (IM7)	Biolegend	Cat# 103026, RRID: AB_493713
Anti-CD279/PD-1 (RMP1–30)	Biolegend	Cat# 109110, RRID: AB_572017
Anti-CD186/CXCR6 (SA051D1)	Biolegend	Cat# 151109, RRID: AB_2616760
Anti-T-bet (4B10)	Biolegend	Cat# 644817, RRID: AB_11219388
Anti-Eomes (Dan11mag)	Invitrogen	Cat# 12–4875-82, RRID: AB_1603275
Anti-P2X7R (1F11)	Biolegend	Cat# 148704, RRID: AB_2650952
Anti-Granzyme B Recombinant (QA16A02)	Biolegend	Cat# 372215, RRID: AB_2728382
Anti-CD49a (Ha31/8)	BD Biosciences	Cat# 740262, RRID: AB_2740005
Anti-Ki67 (Rabbit Polyclonal)	Abcam	Cat#ab15580, RRID:AB_443209
Anti-Keratin-5 (Rabbit polyclonal)	Biolegend	Cat#905503, RRID:AB_2734679
Anti-P63	SantaCruz Biotechnology	Cat#sc-25268 PE, RRID:AB_628092
Donkey anti-rabbit Cy-3 secondary	Jackson Immunoresearch	Cat#711–165-152, RRID:AB_2307443
Goat anti-rabbit AF488 secondary	Jackson Immunoresearch	Cat#111–545-144, RRID:AB_2338052

REAGENT or RESOURCE	SOURCE	IDENTIFIER
anti-IFN-g (XMG1.2)	Biolegend	Cat# 505826, RRID:AB_2295770
anti-TNF-a (MP6-XT22)	Biolegend	Cat# 506328, RRID:AB_2562902
anti-IL-2 (JES6–5H4)	Biolegend	Cat# 503808, RRID:AB_315302
anti-mouse CD3e	Biolegend	Cat# 100302, RRID:AB_312667
Bacterial and virus strains		
Lymphocytic choriomeningitis virus (LCMV)- Armstrong strain	Dr. David Masopust, University of Minnesota	N/A
HSV-2 186 kpn (TK−)	Dr. David Masopust, University of Minnesota and Dr. Jennifer Lund, Fred Hutch Cancer Center	N/A
HSV-1K26-GFP	Dr. David Knipe, Harvard University	N/A
HSV-2 333(ZAG)-GFP	Dr. Betsy Herold, Albert Einstein College of Medicine, and Dr. P. Spear, Northwestern University	N/A
Runx3 expressing retrovirus	Dr. J. Justin Milner, Univ. of North Carolina[12]	N/A
Chemicals, peptides, and recombinant proteins		
Collagenase IV	Sigma	Cat# C5138
Dnase I	Sigma	Cat# DN25
Ghost Dye Red 780	Tonbo Biosciences	Cat# 13–0865-T100
H-2Kb -restricted peptide SIINFEKL	Alan Scientific	N/A
H-2Db -restricted LCMV peptide GP33–41	Alan Scientific	N/A
H-2Kb -restricted peptide HSV $gB_{498–505}$ peptide	Alan Scientific	N/A
B-27™ Supplement (50X), serum free	Thermo Fisher Scientific	Cat# 17504044
Y-27632 dihydrochloride	Tocris Biosciences	Cat# 12–541
Mouse EGF Recombinant Protein	PeproTech	Cat#315–09-1MG
CWHM-12	Peter Ruminski, Washington University, St.Louis	N/A
SB431542	Selleck Chemical	Cat#50–797-0
Cultrex BME	R&D Systems	Cat#343201001
Recombinant Mouse B7.1 (CD80)-Fc Chimera	Biolegend	Cat#555406
Recombinant Mouse IL-2	Biolegend	Cat#575408
Recombinant Mouse IL-12	Biolegend	Cat#577002
DAPI (4’,6-Diamidino-2-phenylindole dihydrochloride, 2-(4-Amidinophenyl)-6-indolecarbamidine) dihydrochloride	Sigma	Cat#D9542
H-2Db/GP33–41 KAVYNFATM biotinylated tetramer	NIAID Tetramer core	N/A

REAGENT or RESOURCE	SOURCE	IDENTIFIER
H-2Kb/OVA257–264 SIINFEKL biotinylated tetramer	NIAID Tetramer core	N/A
H-2Kb/HSVgB $_{498–505}$ biotinylated tetramer	NIAID Tetramer core	N/A
Critical commercial assays		
LEGENDplex™ Mouse/Rat Free Active/Total TGF-β1 Assay	Biolegend	Cat#740490
RNeasy Plus Micro Kit	Qiagen	Cat#74034
MojoSort™ Mouse CD8 Naive T cell Isolation Kit	Biolegend	Cat#480044
Deposited data		
Transcriptional comparison of VEO-differentiated CD8 TRM and the CD8 T cells maintained alone	This paper	GEO: GSE249204
Transcriptional comparison of CD8 TRM and TCM in response to HSV-2 infection	This paper	GEO: GSE270942
TCM and TRM signature	Milner et al.[34]	GEO: GSE147080
Experimental models: Cell lines		
Baby hamster kidney-21 cells	ATCC	Catalog# BHK-21 [C-13] (ATCC CCL-10)
Vero cells	ATCC	Catalog# Vero (ATCC CCL-81)
Vaginal epithelial organoid	This paper	N/A
Experimental models: Organisms/strains		
C57BL/6J	The Jackson Laboratory	Catalog# JAX:000664, RRID: IMSR_JAX:000664
B6 CD45.1	The Jackson Laboratory	Catalog# JAX:033076, RRID:IMSR_JAX:033076
B6 Thy1.1	The Jackson Laboratory	Catalog# JAX:000406, RRID: IMSR_JAX:000406
OT-I	The Jackson Laboratory	Catalog# JAX:003831 RRID:IMSR_JAX:003831
P14	Dr. David Masopust, Univ. of Minnesota; Dr. Rafi Ahmed, Emory University	Catalog# MUGEN:M189001, RRID: IMSR_MUGEN:M189001
gBT-1	Dr. Gregoire Lauvau, Albert Einstein College of Medicine, Mueller et al.[56]	N/A
Oligonucleotides		
Axin2_F: CGACCCAGTCAATCCTTATCAC	Ali et al.[18]	N/A
Axin2_R: GGGACTCCATCTACGCTACTG	Ali et al.[18]	N/A
Birc5_F: CCAGGCATGAAGAGTCAGGG	This paper	N/A
Birc5_R: GGCTGCCTGCTTAGAGTTGA	This paper	N/A
Ki67_F: GAGGAGAAACGCCAACCAAGAG	Origene	N/A

REAGENT or RESOURCE	SOURCE	IDENTIFIER
Ki67_R: TTTGTCCTCGGTGGCGTTATCC	Origene	N/A
Sprr1a_F: CAAGGCACCTGAGCCCTGCAA	Origene	N/A
Sprr1a_R: AGGCTCTGGTGCCTTAGGTTGG	Origene	N/A
Krt1_F: GACTCGCTGAAGAGTGACCAGT	Origene	N/A
Krt1_R: GGTCACGAACTCATTCTCTGCG	Origene	N/A
Software and algorithms		
Trimomatic	http://www.usadellab.org/cms/index.php?page=trimmomatic	Trimmomatic (RRID:SCR_011848)
STAR	http://code.google.com/p/rna-star/	STAR (RRID:SCR_004463)
ClusterProfiler	http://bioconductor.org/packages/release/bioc/html/clusterProfiler.html	clusterProfiler (RRID:SCR_016884)
GSEA	http://www.broadinstitute.org/gsea/	Gene Set Enrichment Analysis (RRID:SCR_003199)
Pheatmap	https://www.rdocumentation.org/packages/pheatmap/versions/0.2/topics/pheatmap	pheatmap (RRID:SCR_016418)
Flowjo v10 software	BD Biosciences https://www.flowjo.com/solutions/flowjo	FlowJo (RRID:SCR_008520)
GraphPad Prism v10	GraphPad http://www.graphpad.com/	GraphPad Prism (RRID:SCR_002798)